

# Global sensitivity analysis of bogie dynamics with respect to suspension components

Seyed Milad Mousavi Bideleh<sup>1</sup> · Viktor Berbyuk<sup>1</sup>

Received: 22 May 2014 / Accepted: 10 December 2015 / Published online: 13 January 2016  
© Springer Science+Business Media Dordrecht 2016

**Abstract** The effects of bogie primary and secondary suspension stiffness and damping components on the dynamics behavior of a high speed train are scrutinized based on the multiplicative dimensional reduction method (M-DRM). A one-car railway vehicle model is chosen for the analysis at two levels of the bogie suspension system: symmetric and asymmetric configurations. Several operational scenarios including straight and circular curved tracks are considered, and measurement data are used as the track irregularities in different directions. Ride comfort, safety, and wear objective functions are specified to evaluate the vehicle's dynamics performance on the prescribed operational scenarios. In order to have an appropriate cut center for the sensitivity analysis, the genetic algorithm optimization routine is employed to optimize the primary and secondary suspension components in terms of wear and comfort, respectively. The global sensitivity indices are introduced and the Gaussian quadrature integrals are employed to evaluate the simplified sensitivity indices correlated to the objective functions. In each scenario, the most influential suspension components on bogie dynamics are recognized and a thorough analysis of the results is given. The outcomes of the current research provide informative data that can be beneficial in design and optimization of passive and active suspension components for high speed train bogies.

**Keywords** Multiplicative dimension reduction method · Global sensitivity analysis · Bogie suspension · Safety · Wear · Ride comfort

## 1 Introduction

Railways are known as one of the most prominent means of passenger and goods transportation. High speed, safety, and low pollution are some of the main advantages of rail

---

✉ S.M. Mousavi Bideleh  
[milad.mousavi@chalmers.se](mailto:milad.mousavi@chalmers.se)

V. Berbyuk  
[viktor.berbyuk@chalmers.se](mailto:viktor.berbyuk@chalmers.se)

<sup>1</sup> Department of Applied Mechanics, Chalmers University of Technology, 412 96, Gothenburg, Sweden

transport. An improvement in vehicle bogie dynamics can amend the overall cost efficiency in railway operations. In general, the dynamic performance of high speed train bogies can be investigated from different points of view such as speed, passenger ride comfort, wheel-rail contact wear, and safety factors like maximum track shift force, running stability, and risk of derailment, see, e.g., [1–6]. Various bogie design parameters can directly influence the vehicle performance, and among them primary and secondary suspension components play an important role. In this regard, passive and active suspension systems are developed to fulfill various design requirements. However, different suspension designs might have conflicting effects on the bogie dynamics, and an improvement in one of the objective functions might deteriorate the rest. For example, an increase in speed might reduce safety and comfort levels. Therefore, to achieve higher efficiency from either passive or active suspensions, it is inevitable to formulate and solve several multiobjective optimization problems [7–12].

When it comes to the optimization of complex nonlinear systems, like high speed trains, computation time is a critical issue. To speed up the process, usually a few design parameters and objective functions are introduced to the optimization algorithm. Sensitivity analysis makes it possible to recognize those design parameters that have the most significant influence on the vehicle dynamics. As a result, one can narrow down the number of input design variables for optimization by means of an appropriate sensitivity analysis. Consequently, in order to design new or improve current bogie suspension systems, special attention should be paid to the sensitivity analysis of vehicle's dynamics behavior with respect to different design parameters.

Several studies are done on the sensitivity analysis of rigid and flexible multibody systems with respect to structural parameters such as mass, moment of inertia, also stiffness and damping values, see, e.g., [13–16]. Bestle and Seybold [17] used the adjoint variable method to solve the sensitivity analysis problem of the constrained multibody systems. Sonnevile and Brüls developed sensitivity analysis algorithms for multibody systems based on the direct differentiation method and adjoint variable concepts that required the complete linearization of the dynamics equations of motion and/or the time integration process [18].

Despite the fact that sensitivity analysis is a vital step in bogie suspension design, only a few researches accomplished that so far. Park et al. [19] performed the local sensitivity analysis of a high speed train response with respect to some of the primary and secondary suspension components. Dablin et al. [20] studied the influence of different suspension parameters and equivalent conicity on critical hunting speed of a Chinese high speed passenger train and showed how stability criteria can be improved by using suitable values for design variables. Eom and Lee [21] explored the effects of different parameters on the derailment coefficient and wheel unload ratios of a train model developed in ADAMS/Rail. Suarez et al. [22] examined the safety, ride comfort and track fatigue variations for a railway vehicle by shifting a few suspension stiffness and damping values. However, in the majority of the abovementioned studies, only the local sensitivity analysis has been considered. In other words, the sensitivity has been measured as the partial derivative of the dynamics response with respect to a single variable at a time. Therefore, the domain of input variables was not fully covered using this procedure. Furthermore, for a complex nonlinear system like a high speed train with highly interconnected components and suspension properties that can vary on a wide range, using local sensitivity analysis approaches might be inappropriate [23]. Therefore, it is important to formulate the problem of global sensitivity analysis for this particular purpose.

The Monte Carlo simulation is one of the most common methods for global sensitivity analysis. Mazzola and Bruni [24] used this approach to investigate the effects of the suspension system uncertainty on the critical hunting speed of a railway vehicle. The main

drawback associated with the Monte Carlo simulation is heavy computational effort which makes it unfeasible to be applied to complex systems. Therefore, for sensitivity analysis and optimization of a mechanical system like a high speed train with a large number of degrees of freedom (DOFs) a more computationally efficient algorithm should be utilized.

Analysis of Variance (ANOVA) decomposition or high dimensional model representation (HDMR) decomposes the response function of a high dimensional system into a combination of a set of low dimensional functions and dramatically reduces the computational and sampling efforts [25–28]. This is particularly useful in evaluating the integrals required to determine the global sensitivity indices corresponding to a complex multivariable function. There are several approximations for HDMR expansions, one of the most popular ones is known as cut-HDMR. The component functions in cut-HDMR are evaluated along lines, planes or volumes (i.e., cuts) with respect to a reference point in the sample space. Based on this concept, Zhang and Pandey [29] proposed a multiplicative form of the dimensional reduction method (M-DRM) for global sensitivity analysis. The main advantages of using such approximations are simplicity, high accuracy, computational efficiency, and closed-form representation for the global sensitivity indices. Zhang and Pandey [30] applied this methodology to some mechanical examples and showed that the global sensitivity coefficients obtained are as accurate as those from Monte Carlo simulation, but with a dramatically less computational effort. The same approach is followed here to accomplish the global sensitivity analysis of a one-car railway vehicle dynamics behavior with respect to the suspension components.

In the subsequent sections, the suspension characteristics of the vehicle model developed in multibody dynamics software SIMPACK [31], different operational scenarios as well as the mathematical formulation of safety, ride comfort, and wear objective functions are introduced. Two levels of suspension system configurations are considered: symmetric and asymmetric. In the case of asymmetric vehicle model, the primary (or secondary) stiffness (or damping) values might be different for the right and left hand sides of the vehicle or front and rear wheelsets of the bogies, which makes it possible to investigate the effects of every single suspension element on the bogie dynamics separately. Finally, the M-DRM is applied to achieve the global sensitivity indices for each case. The outcomes of the current study yield useful information regarding the effects of various suspension components on bogie dynamics behavior for different operational scenarios. Such an analysis not only makes it possible to attenuate the number of input parameters for optimization and speed up the process, but also gives insight into design active suspension components in a smarter way.

## 2 Model specification

The one-car vehicle model chosen for the analysis is developed in the multibody dynamics software SIMPACK. The model is composed of a carbody, two bogie frames, and four wheelsets (see Fig. 1). All the aforementioned components are rigid and have a total of six DOFs in space. In addition, eight single DOF journal boxes connect the wheelsets to the bogie frame via a set of primary springs and dampers.

The rail and wheels are created based on the nominal UIC60 and S1002 profiles [31], respectively. The Hertzian theory [32, 33] is applied to evaluate the normal contact force. SIMPACK uses an equivalent-elastic contact search approach that takes the intersection of the wheel and rail profiles and approximates each continuous intersection area by an equivalent contact ellipse. This means that the contact patch's shape is converted into an equivalent ellipse that attains the force values relatively close to those obtained by the actual contact patch. The wheel/rail contact penetration that is required to evaluate the stiffness

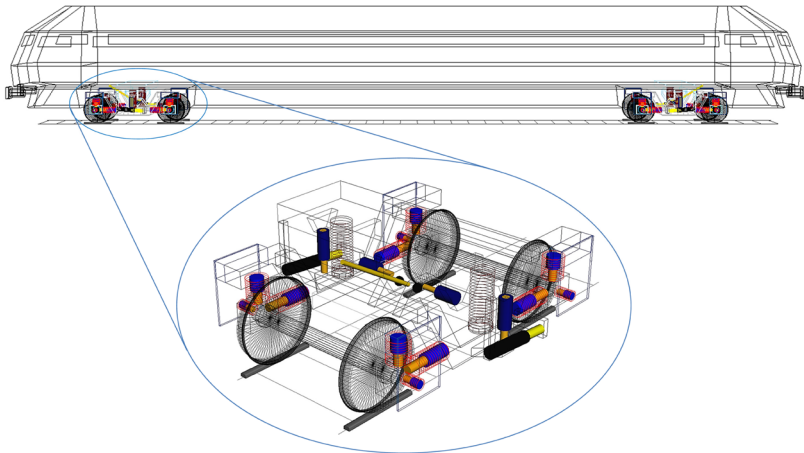


**Fig. 1** One-car vehicle model and bogie suspension components

**Table 1** Suspension system components

Suspension	Springs	Dampers	Anti-Roll bar	Traction-Rod	Bump-Stop
Primary	$k_{lmn}^p$	$c_{lmn}^p$	–	–	–
Secondary	$k_{hmn}^s$	$c_{hmn}^s$	$k_h^{AR}$	$k_h^{TR}$	$k_h^{BS}$

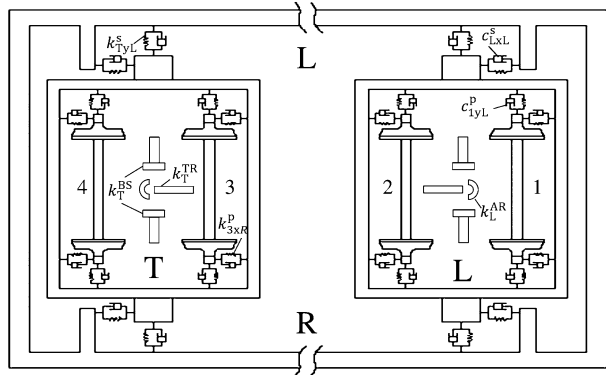
and damping associated with the normal contact force is then approximated based on the distance between the equivalent contact ellipses [31]. Finally, FASTSIM algorithm [34] is employed to provide the tangential contact forces needed to evaluate the wheelset dynamics. It should be noted that a contact search approach using the nonlinear algebraic equations [35] is also considered in a postprocessor stage to calculate wear in this paper, see Sect. 3.3.

The algorithm developed to perform the optimization and sensitivity analysis is implemented in MATLAB. The structural parameters required to specify the vehicle model are stored on the respective input files. These input data files are updated on each iteration. To evaluate the dynamics response and the objective functions of the prescribed railway vehicle model, the SIMPACK time integration solver is executed using the SIMAT module [31] through a MATLAB–SIMPACK co-simulation interface.

### 2.1 Suspension system configuration

Based on the design requirements, different configurations for the bogie suspension can be proposed. Furthermore, passive and active elements can also be integrated to improve the cost efficiency in railway operations. In the current study, the target is to assess the influence of the primary and secondary suspension components on the bogie dynamics behavior. Although all the suspension components are passive here, the sensitivity analysis results can provide beneficial information regarding the design criterion of the active suspensions as well. The bogie primary and secondary suspension components and the corresponding notations are listed in Table 1.

The superscripts p and s denote primary and secondary, respectively. The subscript  $l = 1, 2, 3, 4$  is the wheelset number,  $m = x, y, z$  indicates the longitudinal, lateral and verti-

**Fig. 2** Top view of the carbody

cal directions, respectively. The subscript  $n = R, L$  represents the right or left hand side suspension component and  $h = L, T$  shows leading or trailing bogie, respectively. For instance, parameter  $c_{LXL}^S$  represents the left hand side yaw damper (longitudinal secondary damper) of the leading bogie as shown in Fig. 2. Components  $k_h^{AR}$ ,  $k_h^{TR}$ , and  $k_h^{BS}$ , are modeled as linear springs, torsional springs, and nonlinear spring–damper sets, respectively.

In practice, dampers are usually equipped with elastic bushings at both ends. To take into account the respective effects, all the dampers are modeled as a spring and a damper in series.

## 2.2 Operational scenarios

Speed is a critical issue in evaluating the railway vehicle performance. Higher speeds shorten the journey time and make it possible to reduce the track access charges. Therefore, it is often desired to run the vehicle as fast as possible. Higher speed has some advantages but it might diminish the safety and comfort levels and increase wear. The track radius is another important parameter that can affect the overall performance of the vehicle. A decrease in the path radius of curvature might cause similar problems. Consequently, the ultimate goal of the current research is to perform the sensitivity analysis of the vehicle dynamics response to the suspension components on different operational scenarios.

In this regard, simulations are performed on a wide set of operational scenarios including tracks with different radii ranging from very small radius curve up to straight track. The details of the considered operational scenarios are summarized in Table 2. Rail cant ( $D_t$ ) is defined as the distance between the nominal wheel and rail contact points on the left and right side rails of a track [36]. The vehicle's maximum admissible speed on each case is calculated based on the maximum allowed track plane acceleration, which according to the Swedish Transport Administration (Trafikverket) is  $a_{y,lim} = 0.98 \text{ m/s}^2$  for vehicles with no tilting mechanism [36].

It is assumed that the vehicle runs on a straight line and then on a clothoid transition curved track, before entering the prescribed circular curved scenarios. The lengths corresponding to the tangent and transition curves are 300 and 200 m, respectively. The total simulation time for each scenario and the integration time step are set to be 60 and 0.001 s, respectively.

The measurement data from the Swedish Transport Administration are used as the lateral, vertical, roll, and gauge track irregularities for each particular scenario. The standard deviation of the irregularities are then scaled to provide the worst track condition (QN3) according

**Table 2** Operational scenarios

Scenario	Track type	Radius (m)	Speed (km/h)	Cant $D_t$ (mm)
OS <sub>1</sub>	very small radius	300	88	150
OS <sub>2</sub>	small radius	600	125	150
OS <sub>3</sub>	medium radius	1000	161	150
OS <sub>4</sub>	large radius	3200	263	100
OS <sub>5</sub>	tangent	$\infty$	300	–

to the CEN standard EN 14363 [37]. Therefore, extreme conditions for speed and track irregularities are considered for the analysis. In other words, the speeds below the maximum admissible speed and track conditions smoother than QN3 are not studied in this paper.

### 3 Objective functions

The performance of the underlying railway vehicle is measured based on safety, ride comfort, and wear criteria. As an initial step in formulating the sensitivity analysis problem, it is necessary to express different objective functions in mathematical terms. In most of the cases, this could be done using the available railway standards.

#### 3.1 Safety

A vital criterion that must always be within the permissible design range is safety. This objective function can be investigated from different perspectives. Track shift force, running stability and risk of derailment are the most important safety parameters that are considered here.

##### 3.1.1 Track shift force

Track shift force ( $\sum Y$ ) is measured as the difference between the lateral forces ( $Y$ ) acting on the left and right wheels of a wheelset. High track shift force might deteriorate the track irregularity condition and as a result increase the maintenance cost. According to the CEN standard EN 14363 [37], the limit value for the track shift force is expressed (in kN) as follows:

$$\sum Y_{20 \text{ Hz, } 2 \text{ m, mean, } 99.85 \%} \leq K_1(10 + 2Q_0/3), \quad (1)$$

where  $K_1$  is a constant ( $K_1 = 1$ , for passenger trains) and  $2Q_0$  is the mean static axle load of the vehicle defined as

$$2Q_0 = \frac{m_{\text{veh}}g}{n_a}, \quad (2)$$

where  $m_{\text{veh}}$  is the total mass and  $n_a$  is the number of axles of the vehicle. The final track shift force is equal to the 99.85 % of the value obtained from the forces with a sliding mean over 2 m window in 0.5 m increments and subject to a 20 Hz low-pass filter. The track shift force objective function ( $\Gamma_{\text{TS}}$ ) is then defined as:

$$\Gamma_{\text{TS}} = \max\left(\sum Y_{20 \text{ Hz, } 2 \text{ m, mean, } 99.85 \%}\right), \quad (3)$$

where  $l = 1, 2, 3, 4$  is the axle number (see Fig. 2). Indeed,  $\Gamma_{TS}$  is a scalar which denotes the maximum filtered track shift force among the axles.

### 3.1.2 Running stability

Another important safety criterion is running stability that is particularly important at velocities near the critical hunting speed. The lateral guiding force ( $\sum Y$ ), defined in the previous subsection, can also be used as a measure of the running stability in railway applications.

According to the CEN standard EN 14363 [37], the limit condition for a vehicle to run stably is expressed as:

$$\sum Y_{\text{RMS}, 100 \text{ m}, \text{lim}} = \frac{\sum Y_{\text{max,lim}}}{2} = \frac{K_1(10 + 2Q_0/3)}{2}. \quad (4)$$

A sliding rootmean-square (RMS) of the band-pass filtered guiding force in combination with a 100 m window is applied to attain the final value. The running stability objective function ( $\Gamma_{St}$ ) is then defined as:

$$\Gamma_{St} = \max\left(\sum Y_{\text{RMS}, 100 \text{ m}}\right)_l, \quad l = 1, 2, 3, 4. \quad (5)$$

### 3.1.3 Risk of derailment

Based on the CEN standard EN 14363 [37], the derailment coefficient is defined as the ratio of the lateral ( $Y$ ) to vertical ( $Q$ ) forces acting on each wheel of the vehicle. The safety condition to avoid derailment is defined as:

$$(Y/Q)_{20 \text{ Hz}, 2 \text{ m}, \text{mean}, 99.85 \%} \leq 0.8. \quad (6)$$

The derailment coefficient is calculated as 99.85 % of the sliding mean over a 2 m window of a low-pass filtered signal (with cut-off frequency 20 Hz). The risk of derailment objective function ( $\Gamma_{RD}$ ) is then defined as:

$$\Gamma_{RD} = \max(Y_t/Q_t)_{20 \text{ Hz}, 2 \text{ m}, \text{mean}, 99.85 \%}, \quad (7)$$

in which  $t = 1, 2, \dots, 8$  is the wheel number.

## 3.2 Ride comfort

One of the most important parameters that can influence the overall performance of a railway vehicle is passenger ride comfort. This criterion is often measured based on the carbody accelerations in different directions. Some specific weighting functions are usually applied to the carbody time domain accelerations in order to make the result a better representative of the human body response to external excitations. According to the CEN standard ENV 12299 [38], the ride comfort index ( $N_{MV}$ ) is evaluated in terms of the carbody frequency weighted accelerations in the longitudinal, lateral, and vertical directions as follows:

$$N_{MV} = 6\sqrt{(a_{XP95}^{W_{ad}})^2 + (a_{YP95}^{W_{ad}})^2 + (a_{ZP95}^{W_{ab}})^2}, \quad (8)$$

where  $W_{ad}$  and  $W_{ab}$  are the weighting functions, see [38] for more details. Variables  $a_{XP95}^{W_{ad}}$ ,  $a_{YP95}^{W_{ad}}$ , and  $a_{ZP95}^{W_{ab}}$  represent the 95 % of the RMS value of the frequency weighted accelerations measured at the floor of the carbody in the longitudinal, lateral, and vertical directions, respectively. The ride comfort should be evaluated leastwise at three points, in particular at

**Table 3** Ride comfort classification

$N_{MV} < 1$	Very comfortable
$1 \leq N_{MV} < 2$	Comfortable
$2 \leq N_{MV} < 4$	Medium
$4 \leq N_{MV} < 5$	Uncomfortable
$N_{MV} \geq 5$	Very uncomfortable

the center of the carbody and above each bogie. Table 3 gives the ride comfort classification based on the CEN standard ENV 12299.

The ride comfort objective function ( $\Gamma_C$ ) is then defined as the norm of the ride index at different points of the carbody:

$$\Gamma_C = \sqrt{(N_{MV}^F)^2 + (N_{MV}^M)^2 + (N_{MV}^R)^2}, \tag{9}$$

in which the superscripts F, M, and R represent front, middle, and rear of the carbody, respectively.

### 3.3 Wear

High speed and poor track quality significantly increase the wheel–rail contact wear and maintenance cost. On the other hand, suspension components can affect the wheelset dynamics behavior and wear. It is interesting to explore the effects of suspension components on wear to recognize the most influential elements.

Wear is usually measured as the energy dissipation at the contact patch [39, 40] which is defined as follows:

$$\bar{E} = F_\xi v_\xi + F_\eta v_\eta + M_{\xi\eta} \phi_{\xi\eta}, \tag{10}$$

where  $v_\xi$ ,  $v_\eta$ , and  $\phi_{\xi\eta}$  are the longitudinal, lateral, and spin creepages, and  $F_\xi$ ,  $F_\eta$ , and  $M_{\xi\eta}$  are the corresponding contact forces and torque. The creepages are defined as follows [41]:

$$\begin{cases} v_\xi = \frac{(\dot{\mathbf{r}}^w - \dot{\mathbf{r}}^r)^T \mathbf{t}_1^r}{V}, \\ v_\eta = \frac{(\dot{\mathbf{r}}^w - \dot{\mathbf{r}}^r)^T \mathbf{t}_2^r}{V}, \\ \phi_{\xi\eta} = \frac{(\boldsymbol{\omega}^w - \boldsymbol{\omega}^r)^T \mathbf{n}^r}{V}. \end{cases} \tag{11}$$

The superscripts w and r denote wheel and rail, respectively. Vectors  $\dot{\mathbf{r}}$  and  $\boldsymbol{\omega}$  are the velocity vector of the contact point in the global coordinate system and the angular velocity vector, respectively. Variable  $V$  is the reference velocity. Vectors  $\mathbf{t}_1^r$ ,  $\mathbf{t}_2^r$  are the longitudinal and lateral unit vectors, and  $\mathbf{n}^r$  is the normal unit vector on the rail profile at the contact point.

It is clear that the creepages are functions of the contact point position on the wheel and rail. Therefore, as an initial step in wear calculation, it is necessary to identify the contact point location on the wheel and rail surfaces. Most of the multibody dynamics softwares utilize look-up tables for this purpose. However, a theoretical approach known as the elastic contact formulation using algebraic equations is employed here. In this technique, after parameterization of the wheel and rail surfaces, the contact point coordinates are found by solving a set of four nonlinear algebraic equations, see, e.g., [35, 41–43] for more details.



Once the creepages are attained, one can compute the respective contact forces through a proper contact theory. One of most efficient procedures in this field is FASTSIM algorithm [34]. In this study, the contact search and FASTSIM algorithms are implemented in a post-processing stage to yield the creepages and contact forces, respectively. Finally, the wear objective function ( $\Gamma_W$ ) is defined as:

$$\Gamma_W = \sqrt{\frac{1}{t_f - t_0} \int_{t_0}^{t_f} (|F_{\xi} v_{\xi}| + |F_{\eta} v_{\eta}| + |M_{\xi\eta} \phi_{\xi\eta}|)^2 dt}. \tag{12}$$

Here  $t_0$  and  $t_f$  indicate the initial and final simulation time, respectively.

### 4 Sensitivity analysis

The variance-based sensitivity analysis approach applied in this study is discussed in this section. After a brief introduction about the method, the simplified sensitivity indices are given. Finally, optimization problems formulated to supply an acceptable reference model for the sensitivity analysis are introduced.

#### 4.1 Basic concepts

In general, different objective functions specified in the previous section ( $\Gamma_r$ ,  $r = TS, RD, St, C, W$ ) can be expressed as functions of a set of  $n_d$  independent random design variables  $\mathbf{X} = [x_1, x_2, \dots, x_{n_d}]^T$ , through the respective functional relationship  $\Gamma_r = \mathcal{F}_r(\mathbf{X})$ . Here  $\mathbf{X}$  is a vector of bogie suspension parameters, i.e., stiffness and damping values in this study.

Based on the ANOVA decomposition concept [27, 44], the function  $\mathcal{F}_r(\mathbf{X})$  can be represented as:

$$\mathcal{F}_r(\mathbf{X}) = \mathcal{F}_r^0 + \sum_i \mathcal{F}_r^i(x_i) + \sum_{i < j} \mathcal{F}_r^{ij}(x_i, x_j) + \dots + \mathcal{F}_r^{12\dots n_d}(x_1, x_2, \dots, x_{n_d}), \tag{13}$$

if the function components in (13) are orthogonal and can be expressed as integrals of  $\mathcal{F}_r(\mathbf{X})$ . The following relations can be defined by squaring (13) and integrating over the domain of the input variables [45]:

$$V_{\mathcal{F}_r} = \int (\mathcal{F}_r)^2 d\mathbf{X} - (\mathcal{F}_r^0)^2, \tag{14}$$

$$V_{i_1 \dots i_s} = \int (\mathcal{F}_r^{i_1 \dots i_s})^2 dx_{i_1} \dots dx_{i_s}, \tag{15}$$

where  $1 \leq i_1 < \dots < i_s \leq n_d$ . The constants  $V_{\mathcal{F}_r}$  and  $V_{i_1 \dots i_s}$  are called variances of  $\mathcal{F}_r$  and  $\mathcal{F}_r^{i_1 \dots i_s}$ , respectively. The global sensitivity indices are defined as follows:

$$S_{i_1 \dots i_s} = \frac{V_{i_1 \dots i_s}}{V_{\mathcal{F}_r}}. \tag{16}$$

The integer  $s$  is usually referred as the order or dimension of the sensitivity index. It should be noted that

$$V_{\mathcal{F}_r} = \sum_{s=1}^{n_d} \sum_{i_1 < \dots < i_s} V_{i_1 \dots i_s}. \tag{17}$$

In a similar manner, the variance and global sensitivity index corresponding to a subset  $\mathbf{X}' = [x_{j_1}, x_{j_2}, \dots, x_{j_z}]^T \subseteq \mathbf{X}$ ,  $1 \leq j_1 < \dots < j_z \leq n_d$  are defined by Eqs. (18) and (19), respectively:

$$V_{\mathbf{X}'} = \sum_{s=1}^z \sum_{(i_1 < \dots < i_s) \in J} V_{i_1 \dots i_s}, \tag{18}$$

$$S_{\mathbf{X}'} = \frac{V_{\mathbf{X}'}}{V_{\mathcal{F}_r}}. \tag{19}$$

Here  $J = [j_1, \dots, j_z]$ . Assuming that  $\mathbf{X}''$  is an absolute complement of  $\mathbf{X}'$ , the total variance and sensitivity index associated with the subset  $\mathbf{X}'$  are respectively defined as follows [45]:

$$V_{\mathbf{X}'}^T = V_{\mathcal{F}_r} - V_{\mathbf{X}''}, \tag{20}$$

$$S_{\mathbf{X}'}^T = \frac{V_{\mathbf{X}'}^T}{V_{\mathcal{F}_r}}, \tag{21}$$

where  $0 \leq S_{\mathbf{X}'} \leq S_{\mathbf{X}'}^T \leq 1$ . The total sensitivity index reflects the total influence of a specific parameter on the system output, including all the possible interactions between that parameter and all the others [46].

### 4.2 Simplified sensitivity indices

The sensitivity indices expressed based on the HDMR method (ANOVA decomposition) require evaluation of high-dimensional integrals. This could be a tough task, especially for complex systems. Therefore, an appropriate approximation is often used to improve the computational efficiency. One of the most effective approaches is cut-HDMR in which the function  $\Gamma_r = \mathcal{F}_r(\mathbf{X})$  is expressed as a superposition of its values on lines, planes and hyperplanes passing through a fixed reference point (cut center) with coordinates  $\mathbf{c} = [c_1, \dots, c_{n_d}]^T$ , see, e.g., [44]. Based on this concept, Zhang and Pandey proposed a multiplicative dimensional reduction method (M-DRM) in which a deterministic function  $\Gamma_r = \mathcal{F}_r(\mathbf{X})$  is approximated as follows [29, 30]:

$$\mathcal{F}_r(\mathbf{X}) \approx [\mathcal{F}_r(\mathbf{c})]^{1-n_d} \cdot \prod_{i=1}^{n_d} \mathcal{F}_r(x_i, \mathbf{c}_{-i}), \tag{22}$$

where  $\mathcal{F}_r(\mathbf{c})$  is a constant and  $\mathcal{F}_r(x_i, \mathbf{c}_{-i})$  denotes the function value for the case that all the inputs except  $x_i$  are fixed at their respective cut point coordinates. The M-DRM (Eq. (22)) is capable of approximating the function  $\Gamma_r = \mathcal{F}_r(\mathbf{X})$  with a satisfactory level of accuracy [29, 30] and is particularly useful for approximating the integrals required for evaluation of the sensitivity indices described in the previous section. Using the M-DRM and following the procedure described in [30], the primary and higher order sensitivity indices (Eqs. (19) and (16), respectively) can be approximated as follows:

$$S_i \approx \frac{\beta_i/\alpha_i^2 - 1}{(\prod_{k=1}^{n_d} \beta_k/\alpha_k^2) - 1}, \tag{23}$$

$$S_{i_1 \dots i_s} \approx \frac{\prod_{k=1}^s (\beta_{i_k}/\alpha_{i_k}^2 - 1)}{(\prod_{k=1}^{n_d} \beta_k/\alpha_k^2) - 1}, \tag{24}$$

where  $\alpha_k$  and  $\beta_k$  are defined as the mean and mean square of the  $k$ th univariate function, respectively, and represented as [30]

$$\left\{ \begin{array}{l} \alpha_k \approx \sum_{l=1}^N w_{kl} \mathcal{F}_r(x_{kl}, \mathbf{c}_{-kl}) \\ \beta_k \approx \sum_{l=1}^N w_{kl} [\mathcal{F}_r(x_{kl}, \mathbf{c}_{-kl})]^2 \end{array} \right. , \quad (25)$$

where  $N$  is the total number of the integration points, variables  $x_{kl}$  and  $w_{kl}$  are the  $l$ th Gaussian integration abscissas and the corresponding weight, respectively.

Finally, the total sensitivity index (given by Eq. (21)) corresponding to the  $i$ th parameter ( $x_i$ ) can be expressed as

$$S_i^T \approx \frac{1 - \alpha_i^2 / \beta_i}{1 - (\prod_{k=1}^{n_d} \alpha_k^2 / \beta_k)} . \quad (26)$$

The accuracy of the sensitivity indices introduced earlier depends on the number of the integration points used that can be determined via a convergence study [29, 30]. It should be noted that the total number of function evaluations required for calculating the sensitivity indices using this method is only  $n_d \times N$ , where  $n_d$  is the number of design parameters.

Consequently, in order to accomplish the sensitivity analysis of a system output with respect to an input parameter  $X_i$ , a suitable cut point, together with a probability distribution, has to be chosen. Closed form expressions given by Eqs. (23), (24), and (26) are then utilized to attain the sensitivity indices. The efficiency and applicability of this methodology is already proven through some mathematical and mechanical examples [30]. The target here is to apply this method for sensitivity analysis of a high speed train bogie dynamics with respect to suspension components.

### 4.3 Choosing the cut center

An interesting aspect of the cut-HDMR is that in most applications with well-defined physical systems, if the cut-HDMR yields a satisfactory level of convergence, the results are independent of the choice of the cut center  $\mathbf{c}$  [44]. However, two optimization problems are formulated and solved here to assure that the cut center is in a proper condition.

#### 4.3.1 Optimization

The cut center  $\mathbf{c}$  includes the vectors of the bogie primary and secondary stiffness and damping values. For each of the prescribed operational scenarios, two levels of optimization are considered. The details are summarized in Table 4, where vectors  $\mathbf{k}_p$  and  $\mathbf{k}_s$ , respectively, include the primary and secondary stiffnesses, while  $\mathbf{d}_p$  and  $\mathbf{d}_s$  consist of the primary and secondary damping values.

Indeed, the primary and secondary suspension components are optimized with respect to wear and ride comfort, respectively. In both optimization levels, safety criteria are taken as thresholds.

The reason behind formulating such optimization problems is that wear can significantly influence the maintenance cost and track condition. On the other hand, ride quality can directly affect the passengers' feeling. As a result, from industrial and economical perspectives, ride comfort and wear are usually treated as the most important parameters in railway

**Table 4** Details of the optimization problems

Optimization level	Objective function	Design parameters	Thresholds
L <sub>1</sub>	$\Gamma_W$	$\mathbf{k}_p, \mathbf{d}_p$	$\Gamma_{TS}, \Gamma_{St}, \Gamma_{RD}$
L <sub>2</sub>	$\Gamma_C$	$\mathbf{k}_s, \mathbf{d}_s$	$\Gamma_{TS}, \Gamma_{St}, \Gamma_{RD}$

operations. However, safety objective functions must be always within the admissible limit to assure that the vehicle runs securely.

A genetic algorithm (GA) optimization routine is employed to attain the optimized values of the design parameters at each optimization level, see, e.g., [10, 47, 48] for more information. Since an appropriate initial guess has to be selected for optimization, the in-service values provided by the Bombardier Transportation, Västerås, Sweden are chosen for the first level (L<sub>1</sub>). It should be noted that the optimized values of the design parameters achieved from the case L<sub>1</sub> are applied as the input primary components to the vehicle model for the second level (L<sub>2</sub>) inasmuch as those values are already optimized and help GA to find a better solution.

The optimization outcomes yield the primary and secondary suspension properties that can result in wear reduction, suitable ride comfort as well as acceptable safety levels on each operational scenario. The cut center is then chosen as  $\mathbf{c} = [\mathbf{k}_p^*, \mathbf{d}_p^*, \mathbf{k}_s^*, \mathbf{d}_s^*]^T$  which includes the vectors of the optimized primary and secondary stiffness and damping characteristics. In the subsequent parts of this paper, the superscript (\*) denotes the optimized value of the design parameters.

## 5 Results

In this section, first the optimization results necessary for choosing the cut center are presented. A convergence study is then performed to determine the number of the Gaussian integration abscissas required for the sensitivity analysis to provide acceptable results. Finally, the global sensitivity indices associated with the bogie dynamics behavior with respect to different suspension components are thoroughly rendered and analyzed for two different levels of suspension configurations.

### 5.1 Cut center

As aforementioned in Sect. 4, two levels of optimization (L<sub>1</sub>, L<sub>2</sub>) are formulated to yield the primary and secondary suspension components that minimize wear and ride comfort, respectively.

A vehicle with symmetric suspension configuration is considered for the optimization. This means that every single suspension component has the same value as the corresponding element on the right or left hand side and/or front or rear wheelsets of each bogie. As an example, all the primary longitudinal springs have the same stiffness values in the symmetric vehicle model.

Wear and ride comfort objective functions correlated to in-service ( $\mathbf{c}^0 = [\mathbf{k}_p^0, \mathbf{d}_p^0, \mathbf{k}_s^0, \mathbf{d}_s^0]^T$ ) and optimized input parameters ( $\mathbf{c}^* = [\mathbf{k}_p^*, \mathbf{d}_p^*, \mathbf{k}_s^*, \mathbf{d}_s^*]^T$ ) are compared in Fig. 3.

Since the optimization has been carried out with respect to wear and ride comfort with thresholds on safety (see Sect. 4.3.1), it is clear that at the cut center ( $\mathbf{c}^* = [\mathbf{k}_p^*, \mathbf{d}_p^*, \mathbf{k}_s^*, \mathbf{d}_s^*]^T$ ),

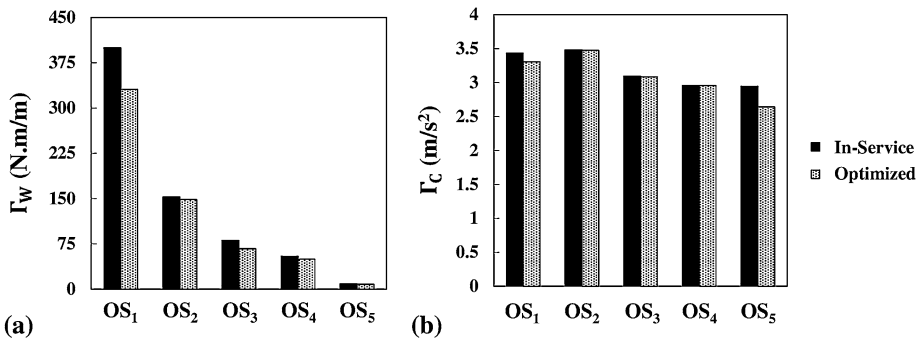


**Fig. 3** Objective function values on different operational scenarios based on the in-service and optimized design parameters: (a) wear ( $\Gamma_W$ ); (b) comfort ( $\Gamma_C$ )

wear and ride comfort are optimized and all the safety objective functions lie within the permissible limit. Therefore, the reference model for the sensitivity analysis is developed based on the optimized values of the suspension parameters obtained from the two optimization levels.

### 5.2 Convergence study

In order to achieve an acceptable approximation of the sensitivity indices using the M-DRM method, it is vital to assess the convergence of the results by increasing the number of Gaussian quadrature integration abscissas.

The first case study is the vehicle with symmetric suspension component configuration. The mean ( $\mu$ ) and coefficient of variation (COV) of the 14 suspension parameters are listed in Table 5. The mean ( $\mu$ ) is chosen equal to the respective cut center value ( $c^*$ ) and the COV is selected in a way that all the objective functions remain within the admissible range for a lognormal distribution of the input variables. It should be noted that for the symmetric vehicle model, for each design parameter the corresponding mean value is equal for all  $l$ ,  $n$  and  $h$ ,  $n$  combinations. For example,  $k_{LxR}^{S*} = k_{LxL}^{S*} = k_{TxR}^{S*} = k_{TxL}^{S*}$ .

All the sensitivity indices in this paper are evaluated based on the Gauss–Hermite quadrature integrals with a lognormal distribution of the input variables; see, e.g., [29, 30, 49] for more details on the numerical procedure.

The convergence analysis of the sensitivity indices corresponding to OS<sub>1</sub> is shown in Fig. 4. It is obvious that for the track shift force ( $\Gamma_{TS}$ ) and risk of derailment ( $\Gamma_{RD}$ ) objective functions,  $N = 5$  integration abscissas are not sufficient (see Fig. 4 (c, e)). However, a satisfactory level of convergence can be achieved by choosing  $N = 9$  or more in all cases.

In Fig. 4, the values  $S_{\Gamma_W}$ ,  $S_{\Gamma_C}$ ,  $S_{\Gamma_{TS}}$ ,  $S_{\Gamma_{St}}$ , and  $S_{\Gamma_{RD}}$  are the primary sensitivity indices for wear, ride comfort, track shift force, running stability and risk of derailment objective functions, respectively.

The number of function evaluations using M-DRM method is merely  $n_d \times N$ . Note that for a specific set of input variables and in each operational scenario, all the objective functions are simultaneously evaluated by a single time integration of the model. The convergence study showed that for a complex system like a high speed train in question (with input suspension parameters given in Table 5), a satisfactory level of sensitivity analysis can be attained with just  $14 \times 9 = 126$  ( $n_d = 14$  design parameters and  $N = 9$  integration abscissas) function evaluations. This is the most prominent aspect of the global sensitivity analysis

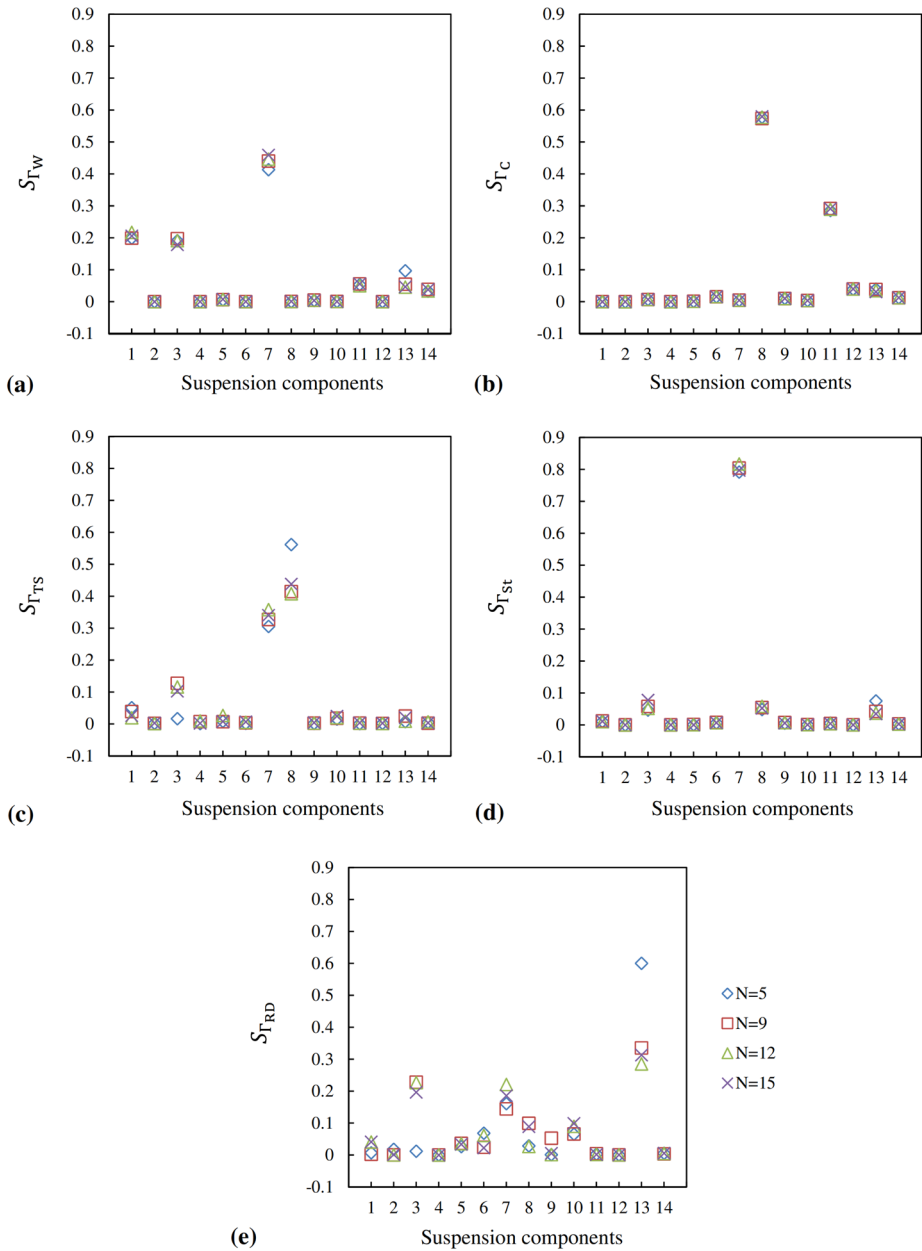


**Fig. 4** Primary sensitivity indices for different objective functions (running on OS<sub>1</sub> scenario): (a)  $S_{\Gamma_W}$ ; (b)  $S_{\Gamma_C}$ ; (c)  $S_{\Gamma_{TS}}$ ; (d)  $S_{\Gamma_{St}}$ ; (e)  $S_{\Gamma_{RD}}$

using this approach, which can dramatically reduce the computational efforts compared to other methods.

In the subsequent sections, the sensitivity analysis is performed for two levels of suspension configurations. At the first step a vehicle with symmetric suspension components

**Table 5** Mean and COV of the symmetric vehicle suspension components

Parameter number	Suspension component	Mean ( $\mu$ )	COV
1	$k_{l_{xn}}^p$	$k_{l_{xn}}^{p*}$	0.5
2	$c_{l_{xn}}^p$	$c_{l_{xn}}^{p*}$	0.5
3	$k_{l_{yn}}^p$	$k_{l_{yn}}^{p*}$	0.3
4	$c_{l_{yn}}^p$	$c_{l_{yn}}^{p*}$	0.5
5	$k_{l_{zn}}^p$	$k_{l_{zn}}^{p*}$	0.5
6	$c_{l_{zn}}^p$	$c_{l_{zn}}^{p*}$	0.5
7	$k_{h_{xn}}^s$	$k_{h_{xn}}^{s*}$	0.5
8	$c_{h_{xn}}^s$	$c_{h_{xn}}^{s*}$	0.5
9	$k_{h_{yn}}^s$	$k_{h_{yn}}^{s*}$	0.5
10	$c_{h_{yn}}^s$	$c_{h_{yn}}^{s*}$	0.5
11	$k_{h_{zn}}^s$	$k_{h_{zn}}^{s*}$	0.5
12	$c_{h_{zn}}^s$	$c_{h_{zn}}^{s*}$	0.5
13	$k_h^{AR}$	$k_h^{AR*}$	0.08
14	$k_h^{TR}$	$k_h^{TR*}$	0.05

( $n_d = 14$  parameters introduced in Table 5) is studied. This type of vehicle is called a symmetric vehicle model in this paper. Finally, a vehicle model with another suspension configuration is analyzed in which all the primary and secondary suspension components on different sides of the vehicle can take dissimilar values. This type of vehicle is referred as an asymmetric vehicle model and makes it possible to scrutinize the sensitivity of bogie dynamics behavior with respect to every single element of the suspension system components. More details on the asymmetric vehicle model are given in Sect. 5.4.

### 5.3 Symmetric vehicle model

The total sensitivity indices for a vehicle model with symmetric suspension components (and design variables listed in Table 5) are shown in Fig. 5 for different operational scenarios. Since Gaussian integration using  $N = 9$  or more points showed satisfactory results (see Fig. 4),  $N = 12$  is chosen for the analysis in this section. Therefore, the number of function evaluations are  $14 \times 12 = 168$  (with  $n_d = 14$  design parameters and  $N = 12$  integration abscissas), for each operational scenario (OS<sub>1</sub>–OS<sub>5</sub>).

#### 5.3.1 Wear

From Fig. 5 it can be deduced that the primary longitudinal and lateral springs ( $k_{l_{xn}}^p$ ,  $k_{l_{yn}}^p$ , i.e., parameters no. 1, 3 in Table 5) as well as longitudinal secondary springs  $k_{h_{xn}}^s$  (parameter no. 7) have the most important influence on wear. This means that the wear total sensitivity index ( $S_{I_w}^T$ ) reflects higher values with respect to those parameters, see Fig. 5(a) for a symmetric vehicle running on very small radius curves (OS<sub>1</sub>). However, as the vehicle's speed

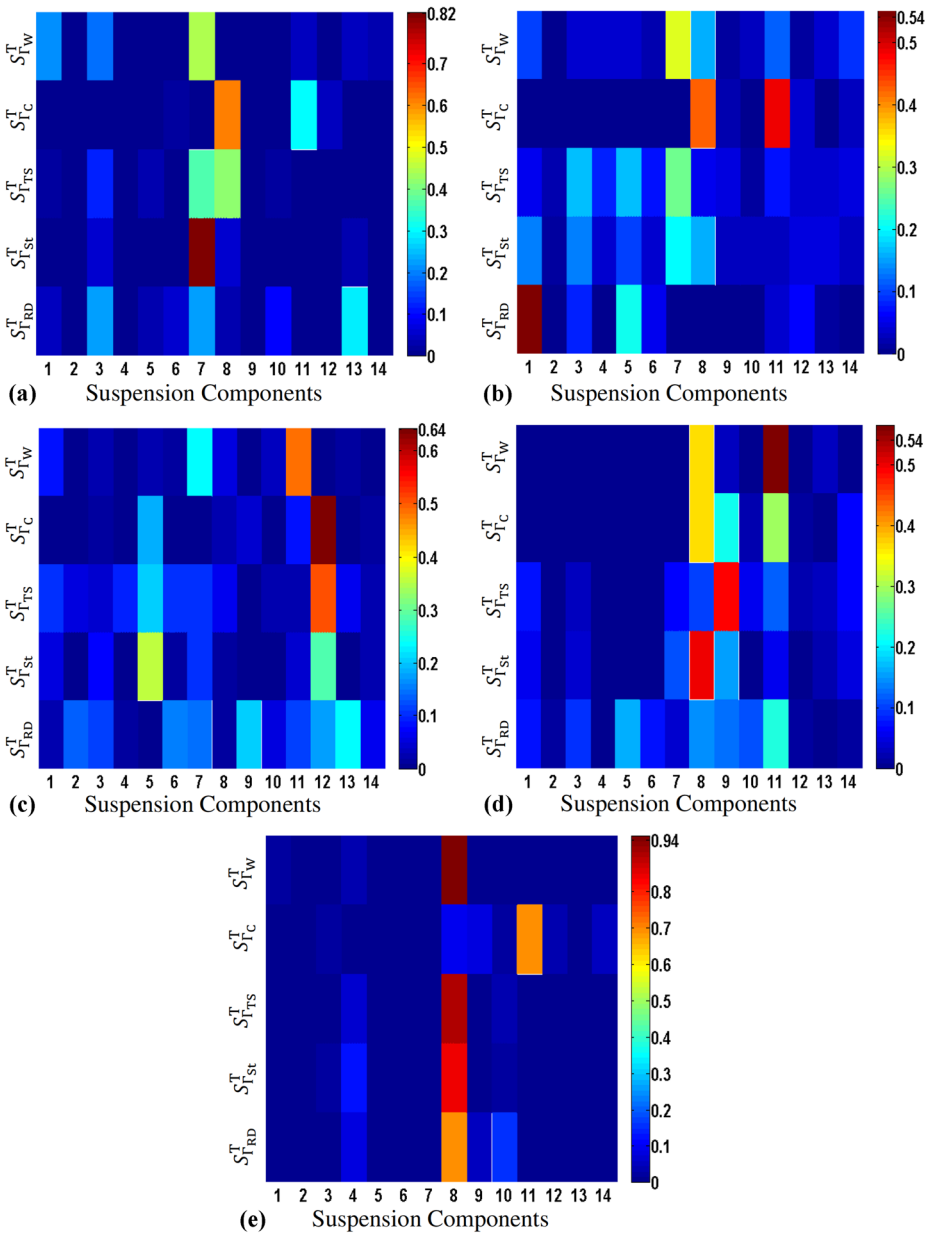


**Fig. 5** Total sensitivity indices associated with different objective functions: (a) OS<sub>1</sub>; (b) OS<sub>2</sub>; (c) OS<sub>3</sub>; (d) OS<sub>4</sub>; (e) OS<sub>5</sub>

and the track curve radii increase, the effects of yaw dampers  $c_{hxn}^s$  (parameter no. 8) and secondary vertical springs  $k_{hzn}^s$  (parameter no. 11) become dominant, see Figs. 5 (b)–(e).

This could be interpreted as follows: on very small radius curves (OS<sub>1</sub>), choosing suitable values of the longitudinal and lateral primary springs ( $k_{ixn}^p, k_{iyx}^p$ ) might make it easier for the wheelset to take a radial position in the track and as a result reduce wear. Furthermore,



in such operational scenarios, the longitudinal secondary springs  $k_{\text{hxn}}^s$  control the carbody vibrations. Therefore, proper values for those parameters might reduce the corresponding unpleasant effects on the bogie dynamics and wear. However, as the speed and radius of curvature increase, the vertical carbody motion become dominant, and a suitable set of vertical secondary springs  $k_{\text{hzn}}^s$  is required to reduce the effects of the carbody motions on the bogie dynamics.

Another interesting outcome is that for a large radius of curvatures and tangent track (OS<sub>4</sub> and OS<sub>5</sub>) the impressions of the longitudinal secondary springs  $k_{\text{hxn}}^s$  become less important while, the yaw dampers' effects on wear become conquering (Figs. 5 (d)–(e)). This shows that for operational scenarios with a large radius of curvature, the bogie dynamics is mostly affected by the yaw dampers  $c_{\text{hxn}}^s$ .

### 5.3.2 Ride comfort

From Fig. 5 it is clear that in almost all the prescribed operational scenarios (OS<sub>1</sub>–OS<sub>5</sub>), yaw dampers  $c_{\text{hxn}}^s$  and vertical secondary springs  $k_{\text{hzn}}^s$  (parameters no. 8, 11 in Table 5, respectively) are the most influential parameters on the passenger ride comfort inasmuch as the ride comfort total sensitivity index ( $S_{TC}^T$ ) showed higher values with respect to those particular elements. This is a proper evidence for developing advanced types of suspension such as vertical air springs in modern bogie designs for high speed trains.

In addition, the sensitivity analysis showed that yaw dampers  $c_{\text{hxn}}^s$  can significantly affect the carbody vibrations, and higher qualities of ride comfort can be obtained by choosing convenient values of the yaw dampers. It can also be deduced that other suspension parameters cannot substantially affect ride comfort. Such a conclusion could be really useful in narrowing down the number of input parameters and reducing the computational efforts once dealing with optimization problems with respect to ride comfort.

### 5.3.3 Safety

In this paper, the difference between the lateral forces acting on the left and right wheels of a wheelset is the basis of evaluation of the safety objective functions ( $\Gamma_{TS}$ ,  $\Gamma_{St}$ , and  $\Gamma_{RD}$ ). Therefore, the sensitivity analyses of all the safety criteria are simultaneously investigated.

For those operational scenarios that the vehicle runs on curves (OS<sub>1</sub> to OS<sub>4</sub>), the safety objective functions are mostly sensitive to the primary longitudinal and lateral springs ( $k_{\text{lxn}}^p$ ,  $k_{\text{lyn}}^p$ , i.e., parameters no. 1, 3 in Table 5) which is understandable inasmuch as those parameters can affect the lateral motion of the wheelsets on curves, see Fig. 5(a)–(d). Furthermore, it should be noted that for some operational scenarios (OS<sub>2</sub> and OS<sub>4</sub>, for example), the risk of derailment is also sensitive to the vertical primary springs  $k_{\text{lzn}}^p$  and dampers  $c_{\text{lzn}}^p$  (parameters no. 5, 6 in Table 5, respectively). Such a conclusion is reasonable, since the vertical force acting on each wheel can affect the risk of derailment evaluation, see Eq. (7).

When it comes to the secondary suspension components and the respective effects on safety criteria, it is unfeasible to draw a general conclusion whereof the system is highly nonlinear, and it is uneasy to relate the secondary suspension components to the total lateral forces acting on each of the wheelsets. Although, in most of the scenarios, the longitudinal secondary springs  $k_{\text{hxn}}^s$  as well as yaw dampers  $c_{\text{hxn}}^s$  can have noticeable effects on safety issues (see, e.g., Fig. 5(a), (b), and (d)). This is in agreement with the previous conclusions concerning wear objective function (which is evaluated based on the wheelset movements and contact forces).

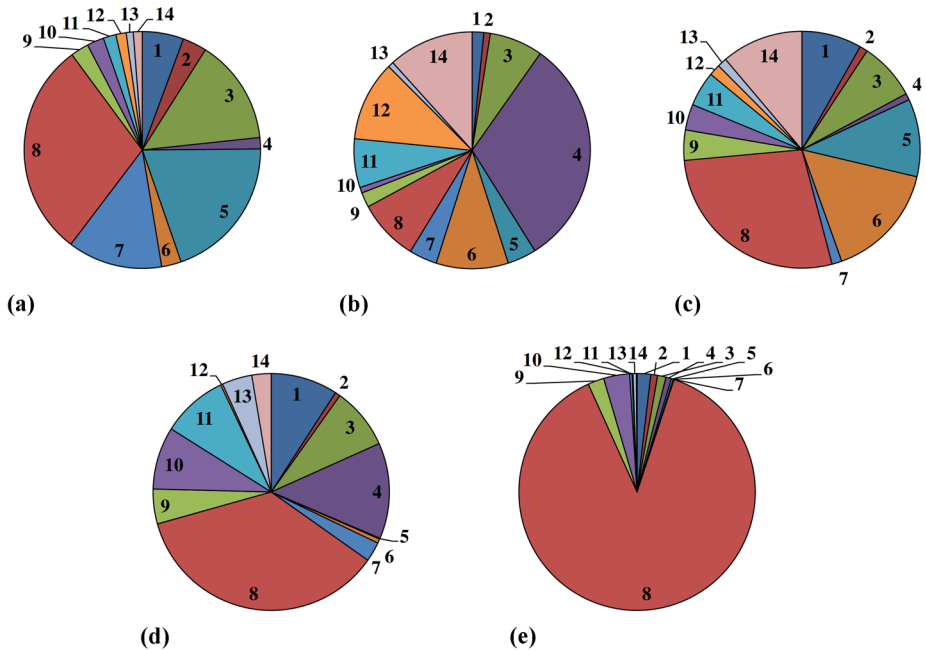


**Fig. 6** Track shift force total sensitivity index ( $S_{\Gamma_{TS}}^T$ ) with respect to the suspension components for the leading axle of the symmetric vehicle running on: (a) OS<sub>1</sub>; (b) OS<sub>2</sub>; (c) OS<sub>3</sub>; (d) OS<sub>4</sub>; (e) OS<sub>5</sub>

In the case of a straight line (OS<sub>5</sub>), since the track is symmetric and the speed is below the critical hunting speed, the lateral forces acting on the wheelsets are smaller than those corresponding to a vehicle running on curves. The lateral primary and secondary dampers ( $c_{lyn}^p, c_{hyn}^s$ , i.e., parameters no. 4, 10 in Table 5) as well as yaw dampers  $c_{hxn}^s$  are the most important elements that can influence the safety criteria for a vehicle running on tangent track (OS<sub>5</sub>) since the respective safety total sensitivity indices ( $S_{\Gamma_{TS}}^T, S_{\Gamma_{St}}^T, S_{\Gamma_{RD}}^T$ ) exhibit higher values with respect to those components, see Fig. 5(e). This could be due to the fact that the lateral primary and secondary dampers ( $c_{lyn}^p, c_{hyn}^s$ ) can suppress the lateral motion of the bogie while running on a tangent track.

Based on Eqs. (3), (5), and (7), the track shift force ( $\Gamma_{TS}$ ), running stability ( $\Gamma_{St}$ ), and risk of derailment ( $\Gamma_{RD}$ ) are defined as the maximum respective value among all the wheelsets (wheels, in the case of risk of derailment). This maximum value can occur on any of the wheelsets during the operation which makes it difficult to interpret the sensitivity of the safety objective functions to the suspension components. Therefore, to investigate those effects more specifically, the influence of the suspension components on the safety criteria of the leading axle is considered.

The total sensitivity indices of the track shift force ( $S_{\Gamma_{TS}}^T$ ), running stability ( $S_{\Gamma_{St}}^T$ ), and risk of derailment ( $S_{\Gamma_{RD}}^T$ ) associated with the leading axle with respect to the 14 suspension components listed in Table 5 are shown in Figs. 6, 7, and 8, respectively. Here each sector area represents the respective sensitivity index value.

For a vehicle running on curved tracks (OS<sub>1</sub>–OS<sub>4</sub>), the longitudinal and lateral primary springs ( $k_{lxn}^p, k_{lyn}^p$ , i.e., parameters no. 1, 3 in Table 5), have a relatively uniform constant influence on the track shift force, see Fig. 6(a)–(d). On the other hand, the vertical primary

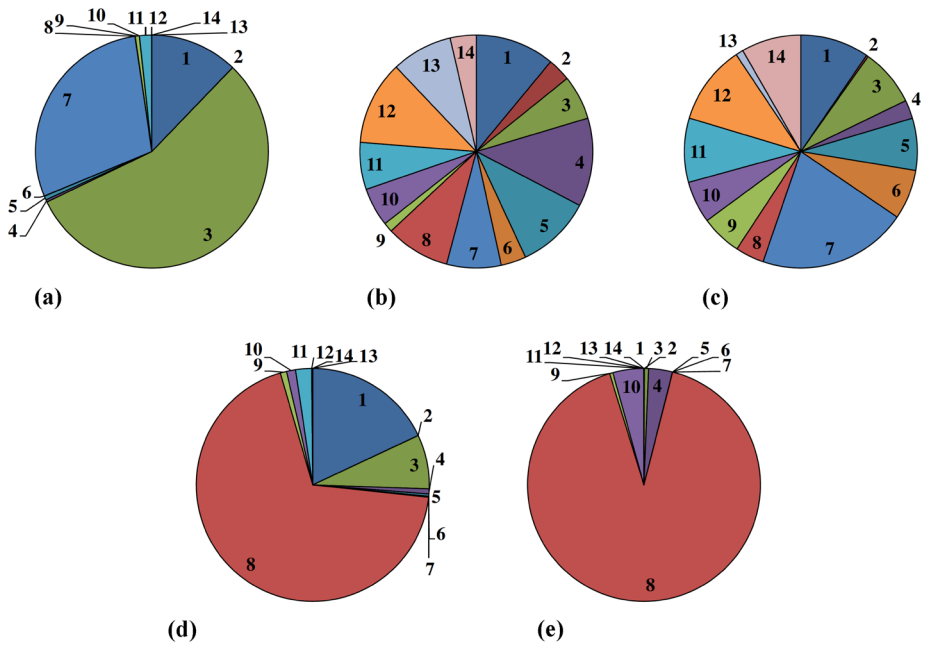


**Fig. 7** Stability total sensitivity index ( $S_{St}^T$ ) with respect to the suspension components for the leading axle of the symmetric vehicle running on: (a) OS<sub>1</sub>; (b) OS<sub>2</sub>; (c) OS<sub>3</sub>; (d) OS<sub>4</sub>; (e) OS<sub>5</sub>

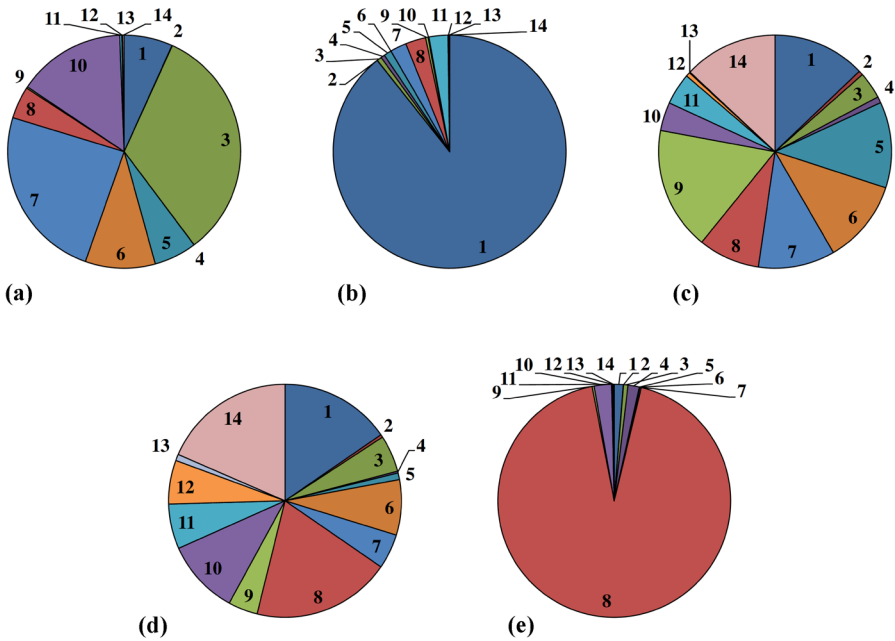


**Fig. 8** Risk of derailment total sensitivity index ( $S_{RD}^T$ ) with respect to the suspension components for the leading axle of the symmetric vehicle running on: (a) OS<sub>1</sub>; (b) OS<sub>2</sub>; (c) OS<sub>3</sub>; (d) OS<sub>4</sub>; (e) OS<sub>5</sub>

springs  $k_{lzn}^p$  (parameter no. 5 in Table 5) can mostly affect  $\Gamma_{TS}$  on tracks with small and medium radius of curvatures (OS<sub>1</sub>–OS<sub>3</sub>).

In some particular scenarios, the lateral and vertical primary dampers ( $c_{lyn}^p$ ,  $c_{lzn}^p$ , i.e., parameters no. 4, 6) have remarkable effects on  $\Gamma_{TS}$ . This could be due to the nature of the track irregularities associated with those scenarios and the ability of the abovementioned dampers in wheelset vibration control in those cases. In the case of secondary suspension, yaw dampers  $c_{hxn}^s$  (parameter no. 8 in Table 5) have the most significant effects on the track shift force, especially for the large radius and straight tracks (Fig. 6).

Similar to the previous case, the longitudinal and lateral primary springs ( $k_{lxn}^p$ ,  $k_{lyn}^p$ ) can remarkably affect  $\Gamma_{St}$  on curved scenarios (Fig. 7(a)–(d)). Furthermore, the longitudinal secondary springs  $k_{hxn}^s$  (parameter no. 7 in Table 5) have also significant effects on the running stability of the leading axle while running on the tracks with relatively small and medium radius of curvatures (Fig. 7(a)–(c)). However, for a large radius and straight tracks (OS<sub>4</sub>, OS<sub>5</sub>), the total sensitivity index of stability ( $S_{\Gamma_{St}}^T$ ) shows that running stability is less sensitive to the longitudinal secondary springs  $k_{hxn}^s$ , and the effects of the yaw dampers  $c_{hxn}^s$  become dominant instead (see Fig. 7(d)–(e)).

To some extent the primary springs ( $k_{lxn}^p$ ,  $k_{lyn}^p$ ,  $k_{lzn}^p$ ) and secondary suspension components have remarkable effects on the risk of derailment for the leading axle of a vehicle running on curves, see Fig. 8(a)–(d). However, in the case of OS<sub>2</sub>, the primary longitudinal springs  $k_{lxn}^p$  have the most significant influence on  $\Gamma_{RD}$ . This could be due to the track irregularities and the corresponding effects on the wheelset dynamics while varying the primary longitudinal spring values. Similar to the previous cases, the yaw dampers  $c_{hxn}^s$  are the most influential parameters on  $\Gamma_{RD}$  while running on straight tracks, see Fig. 8(e).

It is clear that for the symmetric vehicle model, the primary longitudinal and lateral springs ( $k_{lxn}^p$ ,  $k_{lyn}^p$ ) as well as the yaw dampers  $c_{hxn}^s$  (i.e., parameters no. 1, 3, and 8 in Table 5) play a prominent role in dynamics behavior of the vehicle. Therefore, several multiobjective optimization problems can be formulated and solved with respect to those parameters to improve the vehicle performance from different points of view (wear/comfort, for example). More importantly, integrating active control techniques and active dampers like magnetorheological (MR) dampers can also be an interesting idea to get higher efficiency especially on large radius and straight tracks.

## 5.4 Asymmetric vehicle model

In addition to the symmetric vehicle model introduced earlier, an asymmetric vehicle model with the suspension components listed in Table 6 is also studied in this paper.

The difference with the symmetric case is that here the suspension elements are not necessarily the same on the right and left hand sides, as well as front and rear wheelsets of each bogie, and they might take different values. As an example, one could have  $k_{lxR}^p \neq k_{lxL}^p$  for the asymmetric model which means that the longitudinal primary springs are not the same on the right and left hand sides of the leading axle.

From Table 6, it is clear that there are 24 primary springs, 24 primary dampers and 28 secondary suspension elements. Therefore, the model includes 76 suspension parameters in total ( $n_d = 76$ ), potentially different from one another. Such a vehicle model makes it possible to separately investigate the effects of every single suspension element on the bogie dynamics.

The total sensitivity indices for the asymmetric vehicle model with input variables listed in Table 6 are depicted in Figs. 9–13 for different operational scenarios.

The mean and COV of the input variables are chosen the same as for the corresponding suspension element associated with the symmetric vehicle model (listed in Table 5).

**Table 6** Suspension components of the asymmetric vehicle model

Parameter No.	Primary spring	Primary damper	Secondary suspension
1	$k_{1xR}^P$	$c_{1xR}^P$	$k_{LxR}^S$
2	$k_{1yR}^P$	$c_{1yR}^P$	$c_{LxR}^S$
3	$k_{1zR}^P$	$c_{1zR}^P$	$k_{LyR}^S$
4	$k_{1xL}^P$	$c_{1xL}^P$	$c_{LyR}^S$
5	$k_{1yL}^P$	$c_{1yL}^P$	$k_{LzR}^S$
6	$k_{1zL}^P$	$c_{1zL}^P$	$c_{LzR}^S$
7	$k_{2xR}^P$	$c_{2xR}^P$	$k_{LxL}^S$
8	$k_{2yR}^P$	$c_{2yR}^P$	$c_{LxL}^S$
9	$k_{2zR}^P$	$c_{2zR}^P$	$k_{LyL}^S$
10	$k_{2xL}^P$	$c_{2xL}^P$	$c_{LyL}^S$
11	$k_{2yL}^P$	$c_{2yL}^P$	$k_{LzL}^S$
12	$k_{2zL}^P$	$c_{2zL}^P$	$c_{LzL}^S$
13	$k_{3xR}^P$	$c_{3xR}^P$	$k_{TxR}^S$
14	$k_{3yR}^P$	$c_{3yR}^P$	$c_{TxR}^S$
15	$k_{3zR}^P$	$c_{3zR}^P$	$k_{TyR}^S$
16	$k_{3xL}^P$	$c_{3xL}^P$	$c_{TyR}^S$
17	$k_{3yL}^P$	$c_{3yL}^P$	$k_{TzR}^S$
18	$k_{3zL}^P$	$c_{3zL}^P$	$c_{TzR}^S$
19	$k_{4xR}^P$	$c_{4xR}^P$	$k_{TxL}^S$
20	$k_{4yR}^P$	$c_{4yR}^P$	$c_{TxL}^S$
21	$k_{4zR}^P$	$c_{4zR}^P$	$k_{TyL}^S$
22	$k_{4xL}^P$	$c_{4xL}^P$	$c_{TyL}^S$
23	$k_{4yL}^P$	$c_{4yL}^P$	$k_{TzL}^S$
24	$k_{4zL}^P$	$c_{4zL}^P$	$c_{TzL}^S$
25	–	–	$k_L^{AR}$
26	–	–	$k_L^{TR}$
27	–	–	$k_T^{AR}$
28	–	–	$k_T^{TR}$

For instance,  $\mu(c_{1xR}^P) = \mu(c_{1xL}^P) = \dots = \mu(c_{4xL}^P) = \mu(c_{l_{xn}}^{P*})$ . Therefore, the cut center for the sensitivity analysis of the asymmetric vehicle model is chosen the same as the one corresponding to the symmetric model. The sensitivity analysis is accomplished using  $N = 9$  Gaussian quadrature integration abscissas. Consequently, the number of function evaluations is  $76 \times 9 = 684$  for each of the scenarios shown in Figs. 9–13.

5.4.1 Wear

From Figs. 9–13, the wear total sensitivity indices ( $S_{T_w}^T$ ) show that the wheel–rail contact wear is mostly sensitive to the primary longitudinal and lateral springs ( $k_{l_{xn}}^P, k_{l_{yn}}^P$ ). This is in

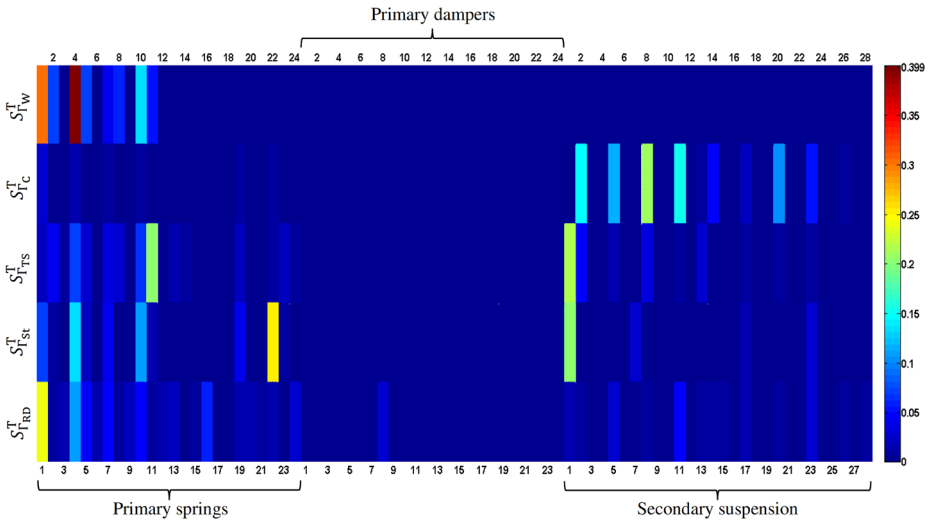


**Fig. 9** Total sensitivity indices for the vehicle running on a curved track with very small radius of curvature (OS<sub>1</sub>)

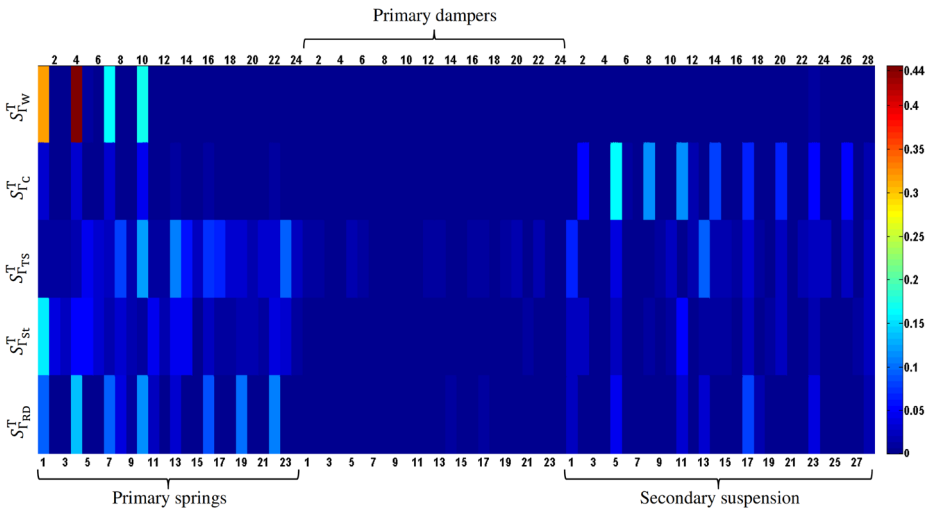


**Fig. 10** Total sensitivity indices for the vehicle running on a curved track with a small radius of curvature (OS<sub>2</sub>)

agreement with the previous conclusion drawn for the symmetric vehicle model. However, unlike the symmetric case, variation of the longitudinal secondary springs  $k_{hxn}^s$  (i.e., parameters no. 1, 7, 13, and 19 of the secondary suspension in Table 6) in the asymmetric model cannot significantly affect the wear objective function.

Such results could be interpreted as follows: in the case of an asymmetric vehicle, variation in one of the four longitudinal secondary springs has smaller influence on wear in contrast to the simultaneous variation of the four respective elements in the symmetric vehicle model. The wear results at the nine integration points for the symmetric and asym-

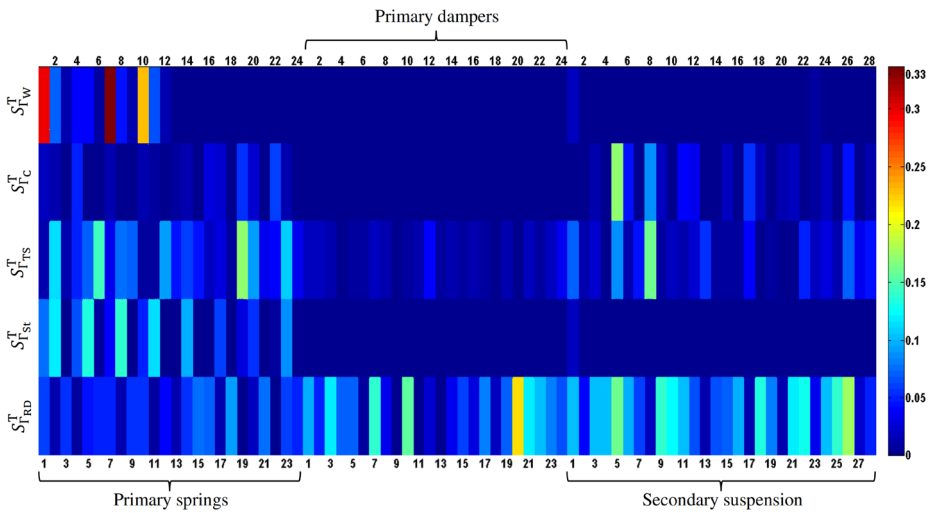


**Fig. 11** Total sensitivity indices for the vehicle running on a curved track with a medium radius of curvature (OS<sub>3</sub>)

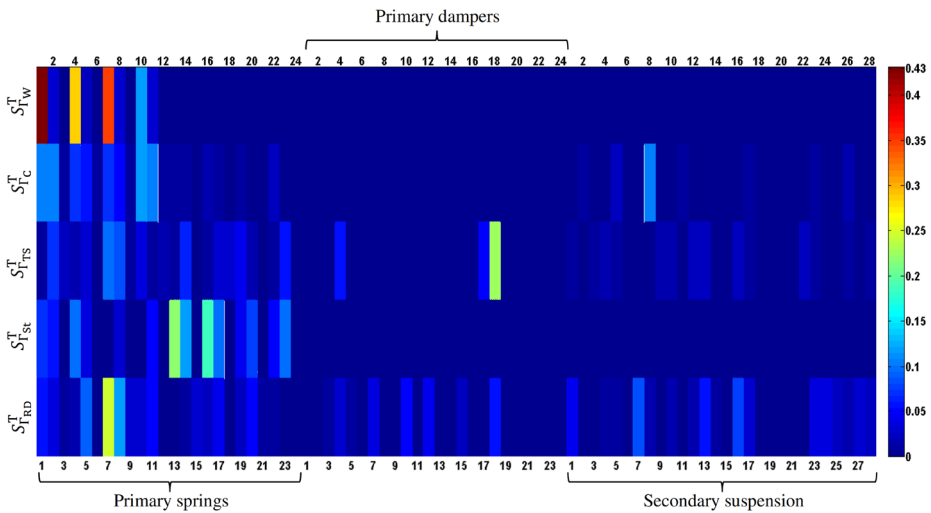


**Fig. 12** Total sensitivity indices for the vehicle running on a curved track with a large radius of curvature (OS<sub>4</sub>)

metric cases are compared in Fig. 14 on a range of the longitudinal secondary springs ( $[\min(k_{hxn}^s) \max(k_{hxn}^s)]$ ). Note that the horizontal axis is on the logarithmic scale.

It is clear that the simultaneous altering of the four longitudinal secondary springs  $k_{hxn}^s$  in the symmetric vehicle model can vary wear on a wider range than in the asymmetric vehicle case in which just one of the longitudinal secondary springs  $k_{hxn}^s$  is changing. Therefore, special attention should be put on design and optimization of the longitudinal secondary springs  $k_{hxn}^s$ , especially in symmetric vehicle models to achieve higher performance.

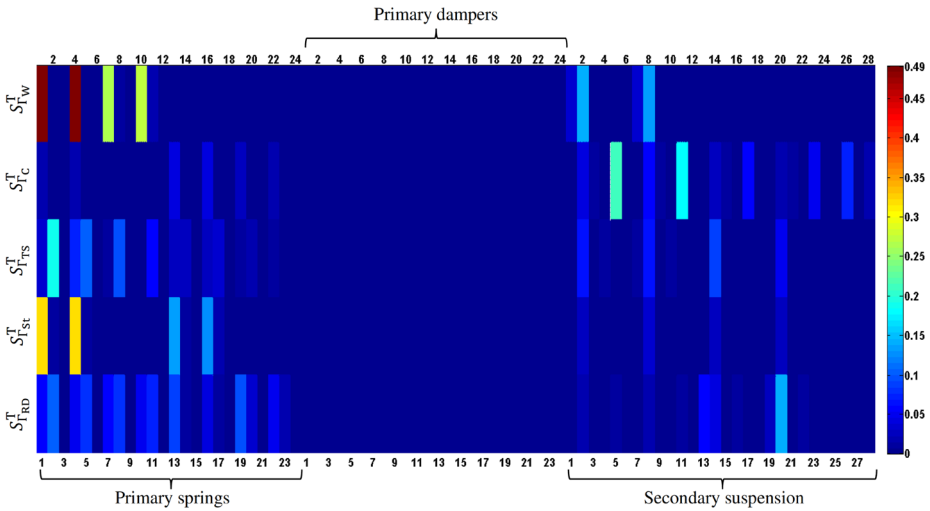
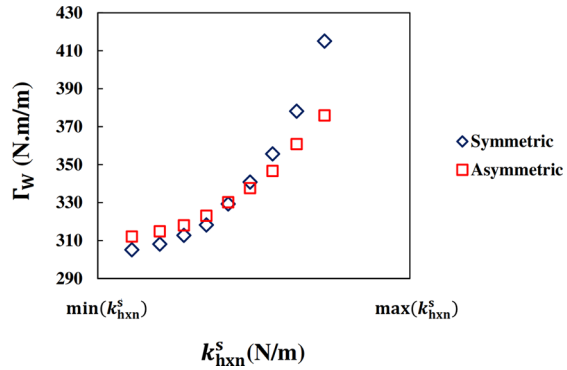


**Fig. 13** Total sensitivity indices for the vehicle running on a tangent track (OS<sub>5</sub>)

**Fig. 14** Wear variation with respect to longitudinal secondary spring



Another interesting result obtained here is that the corresponding suspension components on the right and left hand sides of the vehicle, also front and rear wheelsets of each bogie, might have a totally different effect on wear. For example, for a vehicle operating on a right hand curved track, wear variations with respect to the right and left hand side longitudinal, lateral and vertical primary springs are plotted in Fig. 15(a)–(c).

It is obvious that an increment in the right hand side primary longitudinal and lateral springs ( $k_{lxR}^p, k_{lyR}^p$ ) can reduce wear while the same variation for the left hand side springs ( $k_{lxL}^p, k_{lyL}^p$ ) leads to an opposite result. Note that the wear objective function is measured at the outer wheel of the leading axle (left wheel while running on a right curved track). Therefore, such a combination, i.e., stiffer springs on the right and softer springs on the left, might facilitate the wheelset operation on a curved track and as a result reduce wear.

It is also clear that the vertical primary springs  $k_{lzn}^p$  cannot significantly affect wear, which is in agreement with the result obtained from the sensitivity analysis of the symmetric vehicle model. Therefore, better efficiency (from the wear point of view) can be achieved by



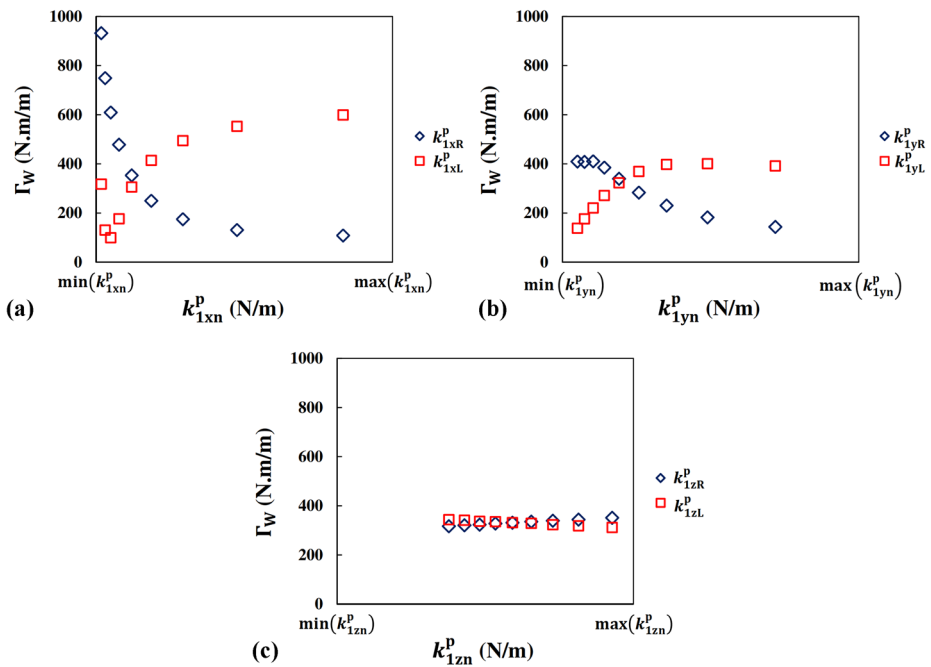


**Fig. 15** Wear variation for OS<sub>1</sub> vs. (a) longitudinal; (b) lateral; (c) vertical primary springs of the leading axle

choosing suitable unequal values for the primary springs of a vehicle when operating in a curved scenario.

### 5.4.2 Ride comfort

From Figs. 9–13, it can be seen that the ride comfort total sensitivity indices ( $S_{I_C}^T$ ) took higher values with respect to the yaw dampers  $c_{hxn}^s$  (parameters no. 2, 8, 14, and 20 of the secondary suspension in Table 6) and vertical secondary springs  $k_{hzn}^s$  (parameters no. 5, 11, 17, and 23 of the secondary suspension in Table 6) which proves the fact that those design parameters are the most influential elements on ride comfort in railway applications.

Such an outcome is in total agreement with the results obtained for sensitivity analysis of the symmetric vehicle model. It should be noted that to some extent the longitudinal primary springs  $k_{1xn}^p$  have also shown some effects on ride quality. However, according to the sensitivity analysis results, the rest of the primary and secondary suspension components do not have a significant effect on ride comfort.

Such information could be particularly useful in attenuating the number of design parameters for the optimization of passive or designing active suspension components to enhance the passenger ride comfort in high speed trains. Therefore, a combination of the optimized passive and/or active vertical secondary springs  $k_{hzn}^s$  as well as yaw dampers  $c_{hxn}^s$  integrated with other passive suspension components might provide a reasonably cheap and efficient passenger ride comfort for railway vehicles. It is also noticeable that although the vehicle is running on a right hand curve on OS<sub>1</sub>–OS<sub>4</sub>, the suspension components attached to the right and left hand sides, also leading and trailing bogies, have more or less the same effects on ride comfort.

### 5.4.3 Safety

All the safety objective functions for the asymmetric model are simultaneously investigated in this section. Similar to the symmetric vehicle model, the primary longitudinal and lateral springs ( $k_{l_{xn}}^p, k_{l_{yn}}^p$ ), as well as the longitudinal secondary springs  $k_{h_{xn}}^s$  and yaw dampers  $c_{h_{xn}}^s$ , play an important role in stability, track shift force, and risk of derailment criteria.

Unlike the symmetric vehicle model, the risk of derailment is not that sensitive to the vertical primary springs  $k_{l_{zn}}^p$  and dampers  $c_{l_{zn}}^p$  inasmuch as at each stage just one vertical primary component is varying in the asymmetric vehicle model at a time.

It is also clear that the safety objective functions cannot be affected by the primary dampers ( $c_{l_{xn}}^p, c_{l_{yn}}^p, c_{l_{zn}}^p$ ) for most of the operational scenarios inasmuch as the respective safety total sensitivity indices ( $S_{I_{TS}}^T, S_{I_{St}}^T, S_{I_{RD}}^T$ ) took small values with respect to those elements (Figs. 9–13). However, there are some changes in the track shift force and risk of derailment sensitivity indices due to the variation of the primary dampers in the case of OS<sub>3</sub> and OS<sub>4</sub> (see Figs. 11, 12). The same result can also be concluded from Fig. 5(c)–(d). This could be due to the track irregularity effects associated with those scenarios and the efficiency of the primary dampers to reduce those unpleasant effects. Consequently, one possible extension of the current research could be to study the sensitivity of different objective functions to the input track irregularities.

Similar to the symmetric vehicle model, it is unfeasible to have a general conclusion regarding the effects of the secondary suspension components on the safety objective functions. However, again the longitudinal secondary springs  $k_{h_{xn}}^s$  (parameters no. 1, 7, 13, and 19 in Table 6) and yaw dampers  $c_{h_{xn}}^s$  (parameters no. 2, 8, 14, and 20 in Table 6) seem to have more considerable effects on safety criteria in comparison with other secondary suspension components. Recall from Eqs. (3), (5), and (7) that safety is measured based on the maximum corresponding safety objective function among all 8 wheels of the vehicle. Since, the maximum value could take place in any of the 4 wheelsets, it is difficult to compare the effects of different suspension components on the vehicle's safety.

The total sensitivity indices associated with the asymmetric vehicle running on a straight track (OS<sub>5</sub>) is shown in Fig. 13. It is clear that the right and left hand side primary and secondary suspension components have the same effects on different objective functions. For example, the wear total sensitivity index ( $S_{I_{W}}^T$ ) has the same values for the design parameters number 1 and 4 from Table 6, i.e., for the right and left hand side longitudinal primary springs ( $k_{l_{xR}}^p$  and  $k_{l_{xL}}^p$ , respectively) that connect the leading axle to the leading bogie frame. This predictable result is due to the symmetry of the track in the case of a straight line (OS<sub>5</sub>).

In order to investigate the effects of different suspension components on bogie safety criteria in a more specific manner, the sensitivity analysis of the leading axle safety with respect to the front bogie suspension components is considered. For different operational scenarios, the total sensitivity indices associated with the track shift force ( $S_{I_{TS}}^T$ ), running stability ( $S_{I_{St}}^T$ ), and risk of derailment ( $S_{I_{RD}}^T$ ) are compared in Figs. 16, 17 and 18, respectively. It should be noted that the numbers assigned to the suspension elements are in agreement with Table 6.

From the safety total sensitivity indices ( $S_{I_{TS}}^T, S_{I_{St}}^T, S_{I_{RD}}^T$ ) given in Figs. 16–18, it can be seen that the primary longitudinal and lateral springs ( $k_{l_{xn}}^p, k_{l_{yn}}^p$ , i.e., primary springs corresponding to the parameters no. 1, 2, 4, 5, 7, 8, 10, and 11 in Table 6) can significantly affect the safety objectives.

In the case of the large radius and straight tracks (OS<sub>4</sub>, OS<sub>5</sub>), the yaw dampers  $c_{h_{xn}}^s$  (parameters no. 2, 8 of the secondary suspension in Table 6) can also remarkably affect the track shift values (see Fig. 16). Since the track shift force and running stability total

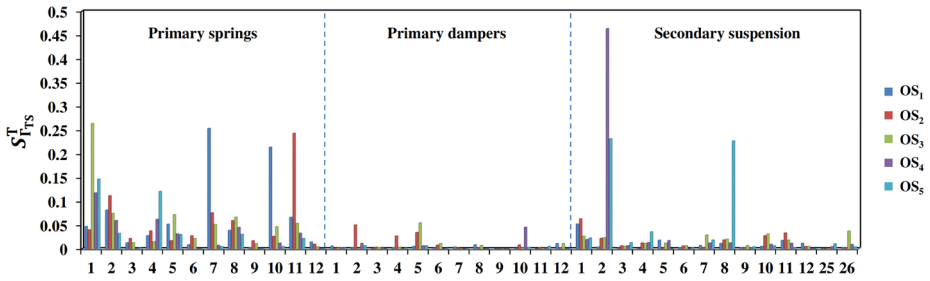


**Fig. 16** The track shift force total sensitivity index ( $S_{ITS}^T$ ) with respect to the suspension components for the leading axle of the asymmetric vehicle

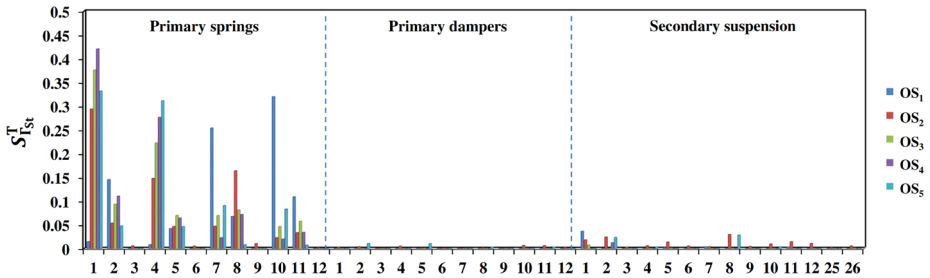


**Fig. 17** The running stability total sensitivity index ( $S_{ISt}^T$ ) with respect to the suspension components for the leading axle of the asymmetric vehicle

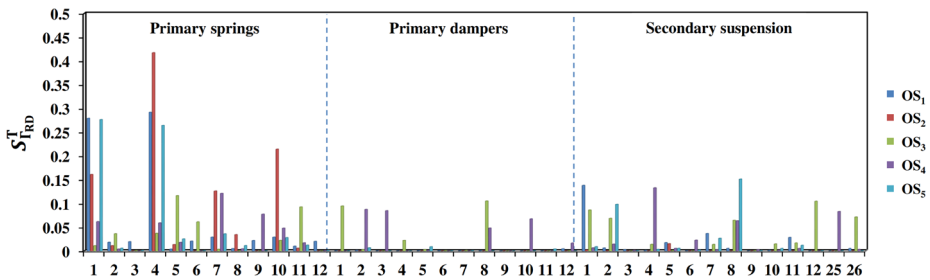


**Fig. 18** The risk of derailment total sensitivity index ( $S_{IRD}^T$ ) with respect to the suspension components for the leading axle of the asymmetric vehicle

sensitivity indices ( $S_{ITS}^T$ ,  $S_{ISt}^T$ ) with respect to the rest of the design parameters are quite small, it can be deduced that those elements have a negligible influence on the track shift force and running stability of the leading axle, see Figs. 16, 17.

Similar conclusions can be drawn for the risk of derailment, see Fig. 18. However, the effects of some of the primary dampers and secondary suspension elements on  $\Gamma_{RD}$  of the leading axle are noticeable on certain operational scenarios.

The sensitivity analysis of the leading axle safety objectives with respect to the suspension components of the asymmetric vehicle model showed that the elements attached to the right and left hand sides, also front and rear wheelsets do not have the same effects on the leading axle safety criteria while operating on curved tracks. This reflects the importance of

using active suspension systems for bogie wheelsets to get the optimum control force and improve the safety performance which can lead to higher speeds, especially on curves.

## 6 Conclusions

The global sensitivity analysis of wear, safety, and ride comfort of a one-car railway vehicle with respect to the bogie suspension components has been scrutinized using the M-DRM. Symmetric and asymmetric configurations of the bogie suspension have been considered. The simulations have been carried out and analyzed for a vehicle running at maximum admissible speed in different operational scenarios.

The current study showed the feasibility and efficiency of the M-DRM for global sensitivity analysis of a multidimensional nonlinear dynamical system (a one-car railway vehicle model with 50 DOFs), which provided the results in a computationally efficient framework. The M-DRM used here revealed practically significant results which can reduce the number of input design parameters for optimization of a bogie suspension system.

Based on the present analysis, the following results have been found to be important:

- Wear is mostly sensitive to the longitudinal and lateral primary springs ( $k_{lxn}^p, k_{lyn}^p$ ). However, for the symmetric vehicle model, as the radius of curvature of the track increases, the effects of the longitudinal and vertical secondary springs ( $k_{hxn}^s, k_{hzn}^s$ ) become dominant. In the case of large radius curves and straight tracks, yaw dampers  $c_{hxn}^s$  can also significantly affect wear.
- Ride comfort is mainly affected by the vertical secondary springs  $k_{hzn}^s$  and yaw dampers  $c_{hxn}^s$ . However, the longitudinal primary springs  $k_{lxn}^p$  have also some influence on ride quality.
- Safety criteria are mostly under the influence of the longitudinal and lateral primary springs ( $k_{lxn}^p, k_{lyn}^p$ ) as well as the longitudinal secondary springs  $k_{hxn}^s$  and yaw dampers  $c_{hxn}^s$ . To some extent, the vertical primary springs  $k_{lzn}^p$  and dampers  $c_{lzn}^p$  can affect the risk of derailment in the case of the symmetric vehicle model.
- Bogies with asymmetric suspension configuration design can potentially reduce wear on curved operational scenarios and as a result attenuate the maintenance cost.
- The sensitivity analysis results obtained in this paper can narrow down the number of the input design parameters for optimization problems of bogie suspension components and improve the computational efficiency.

Finally, active suspension and several multiobjective optimization design problems can be formulated based on the results obtained. Global sensitivity analysis of bogie dynamics with respect to the track irregularities, speed, and wheel conicity could also be a possibility for the future of this work.

**Acknowledgements** The Ekman family foundation is gratefully acknowledged for the financial support of this research. The authors also would like to appreciate Dr. Rickard Persson—Bombardier Transportation, Sweden—for assisting with developing the vehicle model, Dr. Martin Li—Trafikverket, Sweden—who helped us with the track irregularity data, and professor Mikael Enelund—Chalmers University of Technology, Sweden—for his support. Finally, the authors would like to appreciate the anonymous reviewers for their fruitful comments.

## References

1. Peiffer, A., Storm, S., Röder, A., Maier, R., Frank, P.G.: Active vibration control for high speed train bogies. *Smart Mater. Struct.* **14**, 1–18 (2005)

2. Pombo, J., Ambrósio, J., Pereira, M., Lewis, R., Dwyer-Joyce, R., Ariaido, C., Kuka, N.: A study on wear evaluation of railway wheels based on multibody dynamics and wear computation. *Multibody Syst. Dyn.* **24**, 347–366 (2010)
3. Bozzone, M., Pennestrì, E., Salvini, P.: Dynamic analysis of a bogie for hunting detection through a simplified wheel–rail contact model. *Multibody Syst. Dyn.* **25**, 429–460 (2011)
4. Koo, J.S., Cho, H.J.: A method to predict the derailment of rolling stock due to collision using a theoretical wheelset derailment model. *Multibody Syst. Dyn.* **27**, 403–422 (2012)
5. Ignesti, M., Innocenti, A., Marini, L., Meli, E., Rindi, A.: Development of a model for the simultaneous analysis of wheel and rail wear in railway systems. *Multibody Syst. Dyn.* **31**, 191–240 (2014)
6. Nakajima, T., Shimokawa, Y., Mizuno, M., Sugiyama, H.: Air suspension system model coupled with leveling and differential pressure valves for railroad vehicle dynamics simulation. *J. Comput. Nonlinear Dyn.* **9**, 1–9 (2014)
7. He, Y., McPhee, J.: Optimization of curving performance of rail vehicles. *Veh. Syst. Dyn.* **43**(12), 895–923 (2005)
8. He, Y., McPhee, J.: Multidisciplinary optimization of multibody systems with application to the design of rail vehicles. *Multibody Syst. Dyn.* **2005**(14), 111–135 (2005)
9. Johnsson, A., Berbyuk, V., Enelund, M.: Pareto optimisation of railway bogie suspension damping to enhance safety and comfort. *Veh. Syst. Dyn.* **50**(9), 1379–1407 (2012). doi:[10.1080/00423114.2012.659846](https://doi.org/10.1080/00423114.2012.659846)
10. Mousavi Bideleh, S.M., Berbyuk, V.: Multiobjective optimization of a railway vehicle dampers using genetic algorithm. In: *The ASME 2013 International Design Engineering Technical Conferences & Computers and Information in Engineering Conference IDETC/CIE*, Portland, Oregon, USA, 4–7 August 2013 (2013). doi:[10.1115/DETC2013-12988](https://doi.org/10.1115/DETC2013-12988), Paper DETC2013-12988
11. Eberhard, P., Bestle, D., Schiehlen, W.: Optimization of mechanical systems. In: *Advanced Design of Mechanical Systems: From Analysis to Optimization*, pp. 237–252. Springer, Vienna (2009)
12. Jamali, A., Salehpour, M., Nariman-zadeh, N.: Robust Pareto active suspension design for vehicle vibration model with probabilistic uncertain parameters. *Multibody Syst. Dyn.* **30**, 265–285 (2013)
13. Dias, J.M.P., Pereira, M.S.: Sensitivity analysis of rigid–flexible multibody systems. *Multibody Syst. Dyn.* **1**, 303–322 (1997)
14. Ding, J.Y., Pan, Z.K., Chen, L.Q.: Second order adjoint sensitivity analysis of multibody systems described by differential-algebraic equations. *Multibody Syst. Dyn.* **18**, 599–617 (2007)
15. Bhalerao, K.D., Poursina, M., Anderson, K.S.: An efficient direct differentiation approach for sensitivity analysis of flexible multibody systems. *Multibody Syst. Dyn.* **23**, 121–140 (2010)
16. Pi, T., Zhang, Y., Chen, L.: First order sensitivity analysis of flexible multibody systems using absolute nodal coordinate formulation. *Multibody Syst. Dyn.* **27**, 153–171 (2012)
17. Bestle, D., Seybold, J.: Sensitivity analysis of constrained multibody systems. *Arch. Appl. Mech.* **62**, 181–190 (1992)
18. Sonnevile, V., Brüls, O.: Sensitivity analysis for multibody systems formulated on a Lie group. *Multibody Syst. Dyn.* **31**, 47–67 (2014)
19. Park, C., Kim, Y., Bae, D.: Sensitivity analysis of suspension characteristics for Korean high speed train. *J. Mech. Sci. Technol.* **23**, 938–941 (2009). doi:[10.1007/s12206-009-0316-5](https://doi.org/10.1007/s12206-009-0316-5)
20. Dabin, C., Li, L., Xuesong, J., Xinbiao, X., Junjun, D.: Influence of vehicle parameters on critical hunting speed based on Ruzicka model. *Chin. J. Mech. Eng.* **25**(3), 536–542 (2012). doi:[10.3901/CJME.2012.03.536](https://doi.org/10.3901/CJME.2012.03.536)
21. Eom, B.G., Lee, H.S.: Assessment of running safety of railway vehicles using multibody dynamics. *Int. J. Precis. Eng. Manuf.* **11**(2), 315–320 (2010). doi:[10.1007/s12541-010-0036-x](https://doi.org/10.1007/s12541-010-0036-x)
22. Suarez, B., Mera, J.M., Martínez, M.L., Chover, J.A.: Assessment of the influence of the elastic properties of rail vehicle suspensions on safety, ride quality and track fatigue. *Veh. Syst. Dyn.* **51**(2), 280–300 (2013). doi:[10.1080/00423114.2012.725852](https://doi.org/10.1080/00423114.2012.725852)
23. Kraft, S., Puel, G., Aubry, D., Fünfshilling, C.: Improved calibration of simulation models in railway dynamics: application of a parameter identification process to the multi-body model of a TGV train. *Veh. Syst. Dyn.* **51**(12), 1938–1960 (2013). doi:[10.1080/00423114.2013.847467](https://doi.org/10.1080/00423114.2013.847467)
24. Mazzola, L., Bruni, S.: Effect of suspension parameter uncertainty on the dynamic behaviour of railway vehicles. *Appl. Mech. Mater.* **104**, 177–185 (2012). doi:[10.4028/www.scientific.net/AMM.104.177](https://doi.org/10.4028/www.scientific.net/AMM.104.177)
25. Alis, Ö.F., Rabitz, H.: Efficient implementation of high dimensional model representations. *J. Math. Chem.* **29**(2), 127–142 (2001)
26. Li, G., Rosenthal, C., Rabitz, H.: High dimensional model representations. *J. Phys. Chem. A* **105**, 7765–7777 (2001)
27. Sobol', I.M.: Theorems and examples on high dimensional model representation. *Reliab. Eng. Syst. Saf.* **79**, 187–193 (2003)

28. Sudret, B.: Global sensitivity analysis using polynomial chaos expansions. *Reliab. Eng. Syst. Saf.* **93**, 964–979 (2008)
29. Zhang, X., Pandey, M.D.: Structural reliability analysis based on the concepts of entropy, fractional moment and dimensional reduction method. *Struct. Saf.* **43**, 28–40 (2013)
30. Zhang, X., Pandey, M.D.: An effective approximation for variance-based global sensitivity analysis. *Reliab. Eng. Syst. Saf.* **121**, 164–174 (2014)
31. SIMPACK V9.3 documentation. 2013, INTEC GMBH. Wessling, Germany
32. Kalker, J.J.: *Three-Dimensional Elastic Bodies in Rolling Contact*. Kluwer, Dordrecht (1990)
33. Pascal, J.P.: About multi-hertzian-contact hypothesis and equivalent conicity in the case of S1002 and UIC60 analytical wheel/rail profiles. *Veh. Syst. Dyn.* **22**, 57–78 (1993)
34. Kalker, J.J.: A fast algorithm for the simplified theory of rolling contact. *Veh. Syst. Dyn.* **11**, 1–13 (1982)
35. Shabana, A.A., Tobaa, M., Sugiyama, H., Zaazaa, K.: On the computer formulations of the wheel/rail contact problem. *Nonlinear Dyn.* **40**, 169–193 (2005)
36. Andersson, E., Berg, M., Stichel, S.: *Rail Vehicle Dynamics*. Railway Group KTH, Stockholm (2007)
37. CEN, Railway applications—Testing for the acceptance of running characteristics of railway vehicles—Testing for running behaviour and stationary tests, EN 14363. 2005, European Committee for Standardization, Brussels
38. CEN, Railway applications—Ride comfort for passengers—Measurement and evaluation. 1999, European Committee for Standardization, Brussels
39. Pearce, T.G., Sherratt, N.D.: Prediction of wheel profile wear. *Wear* **144**, 343–351 (1991)
40. Bevan, A., Molyneux-Berry, P., Eickhoff, B., Burstow, M.: Development and validation of a wheel wear and rolling contact fatigue damage model. *Wear* **307**, 100–111 (2013)
41. Shabana, A.A., Zaazaa, K.E., Sugiyama, H.: *Railroad Vehicle Dynamics—a Computational Approach*. CRC Press/Taylor & Francis Group, Boca Raton/London (2008)
42. Pombo, J.C., Ambrosio, J.A.C.: Application of a wheel-rail contact model to railway dynamics in small radius curved tracks. *Multibody Syst. Dyn.* **19**, 91–114 (2008)
43. Shabana, A.A., Zaazaa, K.E., Escalona, J.L., Sany, J.R.: Development of elastic force model for wheel/rail contact problems. *J. Sound Vib.* **269**, 295–325 (2004)
44. Rabitz, H., Alis, O.F.: General foundations of high-dimensional model representations. *J. Math. Chem.* **25**, 197–233 (1999)
45. Sobol', I.M.: Global sensitivity indices for nonlinear mathematical models and their Monte Carlo estimates. *Math. Comput. Simul.* **55**, 271–280 (2001)
46. Homma, T., Saltelli, A.: Importance measures in global sensitivity analysis of nonlinear models. *Reliab. Eng. Syst. Saf.* **52**, 1–17 (1996)
47. Mousavi Bideleh, S.M., Berbyuk, V.: Optimization of a bogie primary suspension damping to reduce wear in railway operations. In: *The ECCOMAS Multibody Dynamics*, pp. 1025–1034. University of Zagreb, Zagreb (2013)
48. Mousavi-Bideleh, S.M., Berbyuk, V.: Multiobjective optimisation of bogie suspension to boost speed on curves. *Veh. Syst. Dyn.* (2015). doi:[10.1080/00423114.2015.1114655](https://doi.org/10.1080/00423114.2015.1114655)
49. Carnahan, B., Luther, H.A., Wilkes, J.O.: *Applied Numerical Methods*. Wiley, New York (1969)